INTERNATIONAL JOURNAL FOR NUMERICAL METHODS IN ENGINEERING
Int. J. Numer. Meth. Engng (2010)
Published online in Wiley InterScience (www.interscience.wiley.com). DOI: 10.1002/nme.2906

Analytical integrations in 3D BEM for elliptic problems: Evaluation and implementation

A. Salvadori*, †

CeSiA—Centro di studio e ricerca di sismologia applicata e dinamica strutturale, DICATA—Dipartimento di Ingegneria Civile, Architettura, Territorio e Ambiente, Università di Brescia, via Branze 43, 25123 Brescia, Italy

SUMMARY

The present publication deals with 3D elliptic boundary value problems (potential, Stokes, elasticity) in the framework of linear, isotropic, and homogeneous materials. Numerical approximation of the unique solution is achieved by 3D boundary element methods (BEMs). Adopting polynomial test and shape functions of arbitrary degree on flat triangular discretizations, the closed form of integrals that are involved in the 3D BEMs is proposed and discussed. Analyses are performed for all operators (single layer, double layer, hypersingular). The Lebesgue integrals are solved working in a local coordinate system. For singular integrals, both a limit to the boundary as well as the finite part of Hadamard (*Lectures on Cauchy's Problem in Linear Partial Differential Equations*. Yale University Press: New Haven, CT, U.S.A., 1923) approach have been considered. Copyright © 2010 John Wiley & Sons, Ltd.

Received 19 July 2008; Revised 9 March 2010; Accepted 10 March 2010

KEY WORDS: integral equations; boundary elements; analytical integrations; finite part of Hadamard

1. INTRODUCTION

Modeling elliptic problems by means of boundary integral equations (BIEs) and approximating their solution via boundary element methods (BEMs) is firmly established in the academic community as well as in industry. Several stimulating modern applications and research topics can be effectively described via BIEs: to cite but a few, size and location of tumors from temperature measurements [1], mechanics of highly non-linear material behaviors eventually with large strains and rotations [2] as well as strain gradient constitutive laws [3], mechanics of carbon nanotubes composites [4] and dislocations [5].

*Correspondence to: A. Salvadori, CeSiA—Centro di studio e ricerca di sismologia applicata e dinamica strutturale, DICATA—Dipartimento di Ingegneria Civile, Architettura, Territorio e Ambiente, Università di Brescia, via Branze 43, 25123 Brescia, Italy.
†E-mail: alberto.salvadori@ing.unibs.it

Contract/grant sponsor: Italian Ministry of University and Research (MIUR)

Table I. Kernels and their singularities. Here $r=\|\mathbf{r}\|$. CPV stands for Cauchy's Principal Value, whereas HFP for Hadamard's Finite Part.

Kernel	Asymptotical behavior when $\mathbf{r}\to\mathbf{0}$		Denomination of singularity	Nature of 'integrals' when $\mathbf{x}\in\Gamma$	
	2D	3D		Nature	Symbol
G_{uu}	$O(\log(r))$	$O(r^{-1})$	Weak (integrable)	Lebesgue	$\int$
G_{up},G_{pu}	$O(r^{-1})$	$O(r^{-2})$	Strong	CPV	$\fint$
G_{pp}	$O(r^{-2})$	$O(r^{-3})$	Hyper	HFP	$\fint\!\!\!\fint$

The present note aims at providing a closed form for some 'integrals' involved into the BEMs approximation of 3D elliptic problems [6] . Reference is made to linear elasticity for isotropic and homogeneous materials, as a prototype of such a class of problems. Bulk forces in domain Ω are denoted with $\bar{\mathbf{f}}(\mathbf{y})$; the boundary of Ω is termed Γ and is assumed to be Lipschitz and piecewise continuous; displacements $\bar{\mathbf{u}}(\mathbf{y})$ are given on boundary $\Gamma_u\subseteq\Gamma$, whereas tractions $\bar{\mathbf{p}}(\mathbf{y})$ are given on boundary $\Gamma_p\subset\Gamma$; boundary is taken such that $\Gamma_u\cup\Gamma_p=\Gamma$ and $\Gamma_u\cap\Gamma_p=\emptyset$; vector $\mathbf{r}$ is defined by $\mathbf{r}=\mathbf{x}-\mathbf{y}$; vector $\mathbf{d}$ denotes its opposite: $\mathbf{d}=-\mathbf{r}=\mathbf{y}-\mathbf{x}$ (componentwise, $d_l=y_l-x_l$ with $l=1,2,3$).

The boundary integral formulation of Lamé equations [7–11] stems from Somigliana's identity[‡]:

$$\mathbf{u}(\mathbf{x})+\int_\Gamma G_{up}(\mathbf{r};\mathbf{l}(\mathbf{y}))\mathbf{u}(\mathbf{y})\,\mathrm{d}\Gamma_y=\int_\Gamma G_{uu}(\mathbf{r})\mathbf{p}(\mathbf{y})\,\mathrm{d}\Gamma_y+\int_\Omega G_{uu}(\mathbf{r})\bar{\mathbf{f}}(\mathbf{y})\,\mathrm{d}\Omega_y,\quad \mathbf{x}\in\Omega \tag{1}$$

Equation (1) is the boundary integral representation (BIR) of displacements in the interior of Ω. The traction operator can be applied to Somigliana's identity in the interior of Ω, thus obtaining the BIR of tractions on a surface of normal $\mathbf{n}(\mathbf{x})$, $\mathbf{x}\in\Omega$:

$$\mathbf{p}(\mathbf{x},\mathbf{n}(\mathbf{x}))+\int_\Gamma G_{pp}(\mathbf{r};\mathbf{n}(\mathbf{x});\mathbf{l}(\mathbf{y}))\mathbf{u}(\mathbf{y})\,\mathrm{d}\Gamma_y=\int_\Gamma G_{pu}(\mathbf{r};\mathbf{n}(\mathbf{x}))\mathbf{p}(\mathbf{y})\,\mathrm{d}\Gamma_y+\int_\Omega G_{pu}(\mathbf{r};\mathbf{n}(\mathbf{x}))\bar{\mathbf{f}}(\mathbf{y})\,\mathrm{d}\Omega_y \tag{2}$$

Green's functions G_{uu}, G_{up}, G_{pu} and G_{pp} may contain terms of the following kind (see Table I and the expressions of kernels in Appendix A):

$$\frac{d_1^\alpha d_2^\beta d_3^\gamma}{r^{\alpha+\beta+\gamma+s}},\quad \alpha\geqslant 0,\quad \beta\geqslant 0,\quad \gamma\geqslant 0,\quad s=1,2,3 \tag{3}$$

BIEs for the linear elastic problem can be derived from BIRs (1) and (2) by performing the boundary limit[§] $\Omega\ni\mathbf{x}\to\mathbf{x}\in\Gamma$. The limit process triggers off singularities of Green's functions,

[‡]Equation (1) is based on Green's functions G_{uu} and G_{up}. Unfortunately, the notation internationally used for Green's functions is not unambiguous. In this note, it follows from [9]. Accordingly, G_{uu} stands for the Kelvin tensor, which represents components u_i of the displacement vector $\mathbf{u}$ at a point $\mathbf{x}$ due to a unit force concentrated in space (point $\mathbf{y}$) and acting on the unbounded elastic space Ω_∞ in the direction j. Kernel G_{up} is derived from the Kelvin tensor by means of the boundary traction operator. One finds in [9, 12], among others, a detailed description of the physical meaning of all Green's functions involved in this note.

[§]In the traction equation (5), the boundary limit must be taken at a point $\mathbf{x}\in\Gamma$ with a well-defined normal vector $\mathbf{n}(\mathbf{x})$. Strong and hypersingular kernels generate free-terms—with the notation of [13] they will be termed as $\boldsymbol{\chi}^u_\Gamma(\mathbf{x})$ and $\boldsymbol{\chi}^p_\Gamma(\mathbf{x})$—in the limit process such that $\boldsymbol{\chi}^u_\Gamma(\mathbf{x})=\boldsymbol{\chi}^p_\Gamma(\mathbf{x})=\frac{1}{2}\mathbb{1}$ for smooth boundaries [13–19], whereas special care is required for the discrete problem (see again [13]).

DOI: 10.1002/nme

due to terms (3). They have been extensively investigated. Kernel G_{uu}, which appears in the Single Layer Potential operator $V: H^{-1/2}(\Gamma) \to H^{1/2}(\Gamma)$, shows an integrable singularity (named 'weak'); kernels G_{up}, within the Double Layer Potential operator $K: H^{1/2}(\Gamma) \to H^{1/2}(\Gamma)$, and G_{pu}, within the Adjoint Double Layer Potential operator $K': H^{-1/2}(\Gamma) \to H^{-1/2}(\Gamma)$, present a strong singularity $O(r^{-2})$; kernel G_{pp}, which pertains into the Hypersingular Integral Operator $D: H^{1/2}(\Gamma) \to H^{-1/2}(\Gamma)$, shows a singularity $O(r^{-3})$ greater than the dimension of the integral. Assuming boundary Γ to be smooth, the following BIEs come out:

$$\frac{1}{2}\mathbf{u}(\mathbf{x}) + \int\!\!\!\!\!\!-_{\Gamma_p} G_{up}(\mathbf{r};\mathbf{l}(\mathbf{y}))\mathbf{u}(\mathbf{y})\,\mathrm{d}\Gamma_y + \int_{\Gamma_u} G_{up}(\mathbf{r};\mathbf{l}(\mathbf{y}))\bar{\mathbf{u}}(\mathbf{y})\,\mathrm{d}\Gamma_y$$
$$= \int_{\Gamma_u} G_{uu}(\mathbf{r})\mathbf{p}(\mathbf{y})\,\mathrm{d}\Gamma_y + \int_{\Gamma_p} G_{uu}(\mathbf{r})\bar{\mathbf{p}}(\mathbf{y})\,\mathrm{d}\Gamma_y + \int_{\Omega} G_{uu}(\mathbf{r})\bar{\mathbf{f}}(\mathbf{y})\,\mathrm{d}\Gamma_y, \quad \mathbf{x}\in\Gamma \tag{4}$$

$$\frac{1}{2}\mathbf{p}(\mathbf{x}) + \int\!\!\!\!\!\!-_{\Gamma_p} G_{pp}(\mathbf{r};\mathbf{n}(\mathbf{x});\mathbf{l}(\mathbf{y}))\mathbf{u}(\mathbf{y})\,\mathrm{d}\Gamma_y + \int\!\!\!\!\!\!-_{\Gamma_u} G_{pp}(\mathbf{r};\mathbf{n}(\mathbf{x});\mathbf{l}(\mathbf{y}))\bar{\mathbf{u}}(\mathbf{y})\,\mathrm{d}\Gamma_y$$
$$= \int\!\!\!\!\!\!-_{\Gamma_u} G_{pu}(\mathbf{r};\mathbf{n}(\mathbf{x}))\mathbf{p}(\mathbf{y})\,\mathrm{d}\Gamma_y + \int_{\Gamma_p} G_{pu}(\mathbf{r};\mathbf{n}(\mathbf{x}))\bar{\mathbf{p}}(\mathbf{y})\,\mathrm{d}\Gamma_y + \int_{\Omega} G_{pu}(\mathbf{r};\mathbf{n}(\mathbf{x}))\bar{\mathbf{f}}(\mathbf{y})\,\mathrm{d}\Gamma_y, \quad \mathbf{x}\in\Gamma \tag{5}$$

Equation (4) is referred to as 'displacement equation', whereas Equation (5) is named as 'traction equation': they permit to derive the Calderon Projector for the elastostatic operator. After imposing the fulfillment of Equation (4) on the Dirichlet boundary Γ_u and of Equation (5) on the Neumann boundary Γ_p, the following linear boundary integral problem comes out:

$$\begin{bmatrix} V[.] & -K[.] \\ -K'[.] & -D[.] \end{bmatrix} \begin{bmatrix} \mathbf{p}(\mathbf{y}) \\ \mathbf{u}(\mathbf{y}) \end{bmatrix} = \begin{bmatrix} \mathbf{f}^u(\mathbf{x}) & \mathbf{x}\in\Gamma_u \\ \mathbf{f}^p(\mathbf{x}) & \mathbf{x}\in\Gamma_p \end{bmatrix} \tag{6}$$

Integral operators V, K, K', D are defined by comparison in Equations (4), (5), and (6). Vectors $\mathbf{f}^i(\mathbf{x})$, $i = u, p$, that gather all data (i.e. $\bar{\mathbf{p}}$, $\bar{\mathbf{u}}$, $\bar{\mathbf{f}}$) follow:

$$\mathbf{f}^u(\mathbf{x}) = \frac{1}{2}\bar{\mathbf{u}}(\mathbf{x}) - \int_{\Gamma_p} G_{uu}(\mathbf{r})\bar{\mathbf{p}}(\mathbf{y})\,\mathrm{d}\Gamma_y + \int_{\Gamma_u} G_{up}(\mathbf{r};\mathbf{l}(\mathbf{y}))\bar{\mathbf{u}}(\mathbf{y})\,\mathrm{d}\Gamma_y - \int_{\Omega} G_{uu}(\mathbf{r})\bar{\mathbf{f}}(\mathbf{y})\,\mathrm{d}\Omega_y, \quad \mathbf{x}\in\Gamma_u$$

$$\mathbf{f}^p(\mathbf{x}) = -\frac{1}{2}\bar{\mathbf{p}}(\mathbf{x}) + \int\!\!\!\!\!\!-_{\Gamma_p} G_{pu}(\mathbf{r};\mathbf{n}(\mathbf{x}))\bar{\mathbf{p}}(\mathbf{y})\,\mathrm{d}\Omega_y - \int\!\!\!\!\!\!-_{\Gamma_u} G_{pp}(\mathbf{r};\mathbf{n}(\mathbf{x});\mathbf{l}(\mathbf{y}))\bar{\mathbf{u}}(\mathbf{y})\,\mathrm{d}\Omega_y$$
$$+ \int_{\Omega} G_{pu}(\mathbf{r};\mathbf{n}(\mathbf{x}))\bar{\mathbf{f}}(\mathbf{y})\,\mathrm{d}\Omega_y, \quad \mathbf{x}\in\Gamma_p$$

Integral problem (6) can be given the compact form

$$L[\mathbf{z}] = \mathbf{f} \tag{7}$$

DOI: 10.1002/nme

with all terms defined by comparison. Unknown vector $\mathbf{z}$ is made of tractions (Neumann data) $\mathbf{p}$ on the Dirichlet boundary Γ_u and displacements (Dirichlet data) $\mathbf{u}$ on the Neumann boundary Γ_p. Denote with Z_L the domain of L and define bilinear form $\mathscr{A}_L : Z_L \times Z_L \to R$ as

$$\mathscr{A}_L(\mathbf{a},\mathbf{b}) \stackrel{\text{def}}{=} \int_{\Gamma_u} (V[\mathbf{p}^a](\mathbf{x}) - K[\mathbf{u}^a](\mathbf{x}))\mathbf{p}^b(\mathbf{x})\,\mathrm{d}\Gamma_x + \int_{\Gamma_p} (-K'[\mathbf{p}^a](\mathbf{x}) - D[\mathbf{u}^a](\mathbf{x}))\mathbf{u}^b(\mathbf{x})\,\mathrm{d}\Gamma_x \quad (8)$$

It can be proved—starting from the property of reciprocity [7]—that bilinear form $\mathscr{A}_L$ is symmetric:

$$\mathscr{A}_L(\mathbf{a},\mathbf{b}) = \mathscr{A}_L(\mathbf{b},\mathbf{a}) \quad \forall \mathbf{a},\mathbf{b} \in Z_L$$

As a consequence of the mapping properties of operators V and D, problem (6) is uniquely solvable provided that some conditions are fulfilled [20]. The solution is shown to be a critical point of functional

$$\Psi[\mathbf{z}] = \frac{1}{2}\mathscr{A}_L(\mathbf{z},\mathbf{z}) - \int_\Gamma \mathbf{z}(\mathbf{x})\mathbf{f}(\mathbf{x})\,\mathrm{d}\Gamma_x \quad (9)$$

Let $h>0$ be a parameter and let $[\mathbf{p}_h(\mathbf{y}), \mathbf{u}_h(\mathbf{y})]^{\mathrm{T}} \stackrel{\text{def}}{=} \mathbf{z}_h \in Z_{Lh}$ be a (discrete) approximation of the unknown vector field $\mathbf{z}$, denoting with Z_{Lh} a family of finite-dimensional subspaces of Z_L such that

$$\forall \mathbf{z} \in Z_L, \inf_{\mathbf{z}_h \in Z_{Lh}} \|\mathbf{z} - \mathbf{z}_h\| \to 0 \quad \text{as } h \to 0 \quad (10)$$

Discretization (10) allows to transform integral problem (7) into a set of algebraic equations. Two main techniques have been successfully developed to this aim: the collocation (CBEM) [11] and the symmetric Galerkin [9] method (SGBEM).

The CBEM[¶] requires the fulfillment of integral equation (4) onto a selected set of collocation points $\mathbf{x}_i \in \Gamma$. The evaluation of 'integrals'

$$\int_{\Gamma_s} G_{rs}(\mathbf{x}_i - \mathbf{y})\phi_n(\mathbf{y})\,\mathrm{d}\Gamma_y, \quad r = u, s \in \{u, p\} \quad (11)$$

is required, where symbol $\phi_n(\mathbf{y})$ denotes the nth scalar shape function. The SGBEM approximation of (7) consists of finding $\mathbf{z}_h \in Z_{Lh}$ critical point of the function:

$$\Psi[\mathbf{z}_h] = \frac{1}{2}\mathscr{A}_L(\mathbf{z}_h,\mathbf{z}_h) - \int_\Gamma \mathbf{z}_h(\mathbf{x})\mathbf{f}(\mathbf{x})\,\mathrm{d}\Gamma_x$$

By imposing the stationarity of $\Psi[\mathbf{z}_h]$ respect to the set of nodal values, one deals with the integrals of the following form:

$$\int_{\Gamma_r} \phi_k(\mathbf{x}) \int_{\Gamma_s} G_{rs}(\mathbf{x},\mathbf{y})\phi_n(\mathbf{y})\,\mathrm{d}\Gamma_y\,\mathrm{d}\Gamma_x, \quad r,s \in \{u, p\} \quad (12)$$

where $\phi_k(\mathbf{x})$, $\phi_n(\mathbf{y})$ are *scalar* test and shape functions.

[¶] In the modeling of fracture mechanics problems, an insurmountable mathematical difficulty arises in applying the CBEM making use of the displacement equation only (see e.g. [21, 22]). Several special techniques have been devised to overcome this mathematical degeneracy: among others, the special Green's functions methods [23], the zone method [24] and the Dual BEM [25].

DOI: 10.1002/nme

Denoting with Γ_h a flat triangulation of boundary Γ and with $T_j \subset \Gamma_h$ its generic triangle, the paper is devoted to the analytical integration of

$$\int_{T_j} G_{rs}(\mathbf{x}-\mathbf{y})\phi_n(\mathbf{y})\,\mathrm{d}\Gamma_y, \quad r,s \in \{u,p\} \tag{13}$$

when shape functions $\phi_n(\mathbf{y})$ are polynomials of arbitrary degree. When point $\mathbf{x} \in T_j$, integral (13) may not exist in a classical sense. In such cases, the continuity (with respect to $\mathbf{x}$) between Hadamard's finite part (HFP) of divergent integral (13) and the Lebesgue integral is shown. To achieve this aim, the HFP has been directly evaluated as first; further, the limit process to the boundary $\Omega \ni \mathbf{x} \to \mathbf{x} \in \Gamma$ has been performed—see Section 3.

The implementation requires particular care when point $\mathbf{x}$ belongs to the lines that define the sides of T_j, even if $\mathbf{x} \notin \partial T_j$. Section 4.3 deals with the implementation details. Computational effort of analytical integrations is discussed in Section 4.4. Finally, two benchmarks are considered in Section 4.5, in order to check the analytical integrations and the implementation: they conclude the paper.

2. PROBLEM FORMULATION AND MAJOR RESULTS

2.1. Approximation of unknown fields

Let Γ_h be a triangulation of boundary Γ, $T_j \in \Gamma_h$ its generic triangle and $\mathbf{a}_n$ its generic node. Collect in set $\mathscr{T}_n$ all triangles T_j of Γ_h sharing node $\mathbf{a}_n$ (see an example in Figure 1). Assume over T_j a local (lagrangian) basis $\boldsymbol{\varphi}_j := \{\varphi_j^1, \varphi_j^2, \ldots, \varphi_j^{M(j)}\}$ and denote with $\varphi_j^{n(j)}$ the unique element of $\boldsymbol{\varphi}_j$ such that $\varphi_j^{n(j)}(\mathbf{a}_n) = 1$. Piecewise continuous shape functions $\phi_n(\mathbf{x})$ (see Figure 1) are defined as follows:

$$\phi_n \in C^0(\Gamma_h), \quad \mathrm{supp}(\phi_n) = \mathscr{T}_n, \quad \phi_n|_{T_j} = \varphi_j^{n(j)} \tag{14}$$

Discontinuous shape functions $\phi_n(\mathbf{x})$ are taken as elements of local (lagrangian) basis $\boldsymbol{\varphi}_j$.

Consider a direction l. For scalar problems, $l = 1$ will be generally omitted; for vector problems, $l = 1, 2, 3$. Collect in vector $\boldsymbol{\phi}_l^u$ all piecewise continuous shape functions defined by Equation (14) for the discrete approximation $\mathbf{u}_h(\mathbf{y})$ of the Dirichlet field $\mathbf{u}(\mathbf{y})$ relevant to direction l

$$\boldsymbol{\phi}_l^u(\mathbf{y}) = \{\phi_n(\mathbf{y}) | \quad n = 1, 2, \ldots, N_l\} \tag{15}$$

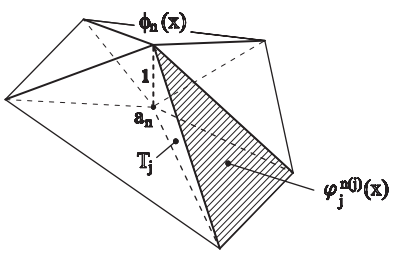

Figure 1. A possible picture of triangle T_j, set $\mathscr{T}_n$, local $\varphi_j^{n(j)}(\mathbf{x})$ and global $\phi_n(\mathbf{x})$ shape functions.

DOI: 10.1002/nme

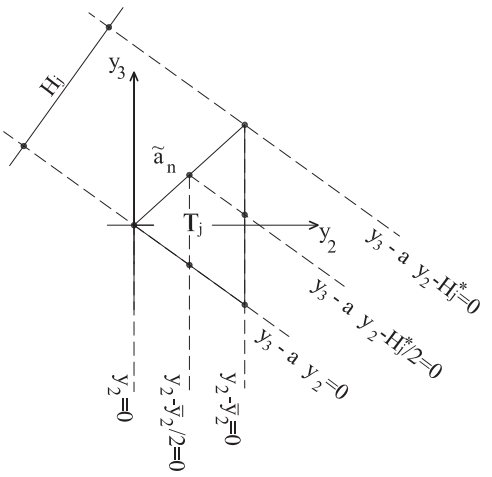

Figure 2. An effective representation for $\varphi_j^{n(j)}$ in local coordinate system $\mathscr{L}$. Here $H_j^* = \sqrt{1+a^2} H_j$. Equation $y_3 - a\, y_2 = 0$ defines the slanting side of triangle T_j, as here depicted. The second slanting side is defined by $y_3 - b\, y_2 = 0$, with $b > a$. Finally, the third side is defined by $y_2 = \bar{y}_2$.

N_l is the number of nodal unknowns in the direction l. Vector $\boldsymbol{\phi}_l^p$ for the discrete approximation $\mathbf{p}_h(\mathbf{y})$ of Neumann field $\mathbf{p}(\mathbf{y})$ relevant to direction l is defined analogously; vector $\boldsymbol{\phi}_l^p$ may contain discontinuous shape functions, depending on the geometry.

Unknown vector fields can be written, therefore, as

$$\mathbf{u}_h(\mathbf{y}) = \sum_l \mathbf{e}_l \otimes \boldsymbol{\phi}_l^u(\mathbf{y}) \hat{\mathbf{u}}_l, \quad \mathbf{p}_h(\mathbf{y}) = \sum_l \mathbf{e}_l \otimes \boldsymbol{\phi}_l^p(\mathbf{y}) \hat{\mathbf{p}}_l \tag{16}$$

In the former equation: (i) tensor product $\otimes : \mathbb{R}^n \times \mathbb{R}^m \to \mathbb{R}^{n \times m}$ is defined as: $(\mathbf{a} \otimes \mathbf{b})\mathbf{c} = (\mathbf{b} \cdot \mathbf{c})\mathbf{a}$; (ii) for vector problems, $\mathbf{e}_l$ is the unit vector in direction l; for scalar problems, it is merely the number 1; (iii) $\hat{\mathbf{u}}_l$, $\hat{\mathbf{p}}_l$ are nodal values for displacements and tractions in direction l.

2.2. *Local basis*

A local coordinate system $\mathscr{L} \equiv \{y_1, y_2, y_3\}$ is defined over triangle T_j in this way: (i) a vertex of T_j is the origin; (ii) plane $y_1 = 0$ contains T_j; (iii) plane $y_3 = 0$ is orthogonal to the side of T_j that does not include the origin. T_j is defined in $\mathscr{L}$ as

$$T_j := \{\mathbf{y} \in \mathbb{R}^3 \text{ s.t. } y_1 = 0;\ 0 < y_2 < \bar{y}_2;\ a y_2 - y_3 < 0;\ b y_2 - y_3 > 0;\ a < b\}$$

Coefficients a and b denote the slope of the two sides of T_j that include the origin (see Figure 2).

Select arbitrarily one of these two sides, say $y_3 - a\, y_2 = 0$. Denote with H_j the height of T_j—see Figure 2. Shape functions $\varphi_j^{n(j)}(\mathbf{y})$ in (15) can be expressed in local reference $\mathscr{L}$ as

$$\varphi_j^{n(j)}(\mathbf{y}) = \mathbf{y}_3^{\mathsf{T}} \Lambda_j^n \mathbf{y}_2 \tag{17}$$

Vectors $\mathbf{y}_3$ and $\mathbf{y}_2$ are defined by

$$\mathbf{y}_3^{\mathsf{T}} = \{1, y_3, y_3^2, \ldots\}, \quad \mathbf{y}_2^{\mathsf{T}} = \{1, y_2, y_2^2, \ldots\}$$

DOI: 10.1002/nme

and matrix Λ_j^n depends on node $\mathbf{a}_n$. For instance, in the six-node element of Figure 2 with reference to node $\tilde{\mathbf{a}}_n$, one writes matrix Λ_j^n as

$$\Lambda_j^n = \begin{bmatrix} 0 & \dfrac{4a}{(a-b)\bar{y}_2} & -\dfrac{4a}{(a-b)\bar{y}_2{}^2} \\ -\dfrac{4}{(a-b)\bar{y}_2} & \dfrac{4}{(a-b)\bar{y}_2{}^2} & 0 \end{bmatrix}$$

In order to solve 'integral' (13), a variable change is worth. For the generic component of vectors $\mathbf{y}_2^{\mathsf{T}}$, $\mathbf{y}_3^{\mathsf{T}}$ in Equation (17), the binomial expansion reads as

$$y_\alpha^i = (x_\alpha + d_\alpha)^i = \sum_{k=0}^{i} \binom{i}{k} x_\alpha^{(i-k)} d_\alpha^k, \quad \alpha = 2, 3$$

with vector $\mathbf{d} = -\mathbf{r} = \mathbf{y} - \mathbf{x}$ (componentwise, $d_\alpha = y_\alpha - x_\alpha$ with $\alpha = 2, 3$) already defined in the introduction. Shape functions $\varphi_j^n(\mathbf{y})$ in (17) can be written as follows:

$$\varphi_j^n(\mathbf{y}) = \mathbf{d}_3^{\mathsf{T}} \mathbf{X}^{(3)\mathsf{T}} \Lambda_j^n \mathbf{X}^{(2)} \mathbf{d}_2 \tag{18}$$

where

$$\mathbf{d}_\alpha^{\mathsf{T}} = \{1, d_\alpha, d_\alpha^2, \ldots\}, \quad \mathbf{X}_{ij}^{(\alpha)} = \binom{i-1}{j-1} x_\alpha^{(i-j)}, \quad i, j = 1, 2, \ldots; \quad \alpha = 2, 3$$

For instance, if one considers linear shape functions, the one referred to the node at the origin reads as[‖]

$$\varphi_j^{n(j)}(\mathbf{y}) = 1 \mathbf{X}^{(3)\mathsf{T}} \begin{bmatrix} 1 & -\dfrac{1}{\bar{y}_2} \end{bmatrix} \mathbf{X}^{(2)} \begin{bmatrix} 1 \\ d_2 \end{bmatrix} \tag{19}$$

with

$$\mathbf{X}^{(2)} = \begin{bmatrix} 1 & 0 \\ x_2 & 1 \end{bmatrix}, \quad \mathbf{X}^{(3)} = [1]$$

2.3. Problem formulation

Integral (13) to be solved comes out by substituting the unknown Dirichlet $\mathbf{u}$ and Neumann $\mathbf{p}$ fields with the discrete approximations (16) into BIEs (4)–(5). By definition (14), 'integral' (13) can be casted in the form as

$$\int_{\mathrm{supp}(\phi_n)} G_{rs}(\mathbf{x}, \mathbf{y}) \phi_n(\mathbf{y}) \, \mathrm{d}\Gamma_y = \sum_j \int_{T_j} G_{rs}(\mathbf{x}, \mathbf{y}) \varphi_j^{n(j)}(\mathbf{y}) \, \mathrm{d}\Gamma_y \stackrel{\mathrm{def}}{=} \sum_j F_{rs}{}_j^n(\mathbf{x}) \tag{20}$$

[‖]Because of the simplicity of form (19), it may be computationally worth for linear shape functions to consider three different local reference systems—one at each vertex—instead of making use of expression (17), what would lead to a more involved matrix Λ_j^n.

DOI: 10.1002/nme

and further simplified in local reference $\mathscr{L}$ as

$$F_{rs}{}_j^n(\mathbf{x}) = \int_{-x_2}^{\bar{y}_2 - x_2} \int_{ad_2+k_a}^{bd_2+k_b} G_{rs}(\mathbf{d}) \mathbf{d}_3^{\mathsf{T}} \, \mathrm{d}d_3 \mathbf{X}^{(3)\mathsf{T}} \Lambda_j^n \mathbf{X}^{(2)} \mathbf{d}_2 \, \mathrm{d}d_2 \tag{21}$$

Coefficient k_a and k_b are defined as $k_a = ax_2 - x_3$ and $k_b = bx_2 - x_3$. The identities $k_a = 0$ and $k_b = 0$ materialize the two sides of T_j that include the origin (see Figure 2).

In the case of linear shape functions, vector $\mathbf{d}_2^{\mathsf{T}} = \{1, d_2\}$ and integral (21) takes the following easy form:

$$F_{rs}{}_j^n(\mathbf{x}) = \int_{-x_2}^{\bar{y}_2 - x_2} \int_{ad_2+k_a}^{bd_2+k_b} G_{rs}(\mathbf{d}) \, \mathrm{d}d_3 \mathbf{d}_2^{\mathsf{T}} \, \mathrm{d}d_2 \begin{bmatrix} 1 - \dfrac{x_2}{\bar{y}_2} \\ \dfrac{1}{\bar{y}_2} \end{bmatrix} = \mathbb{K}_{rs}(\mathbf{x}) \begin{bmatrix} 1 - \dfrac{x_2}{\bar{y}_2} \\ \dfrac{1}{\bar{y}_2} \end{bmatrix} \tag{22}$$

For scalar problems $F_{rs}{}_j^n(\mathbf{x})$ is a scalar function, whereas $\mathbb{K}_{rs}$ is a vector of dimension 2. For vector problems, $F_{rs}{}_j^n(\mathbf{x})$ is a matrix of the same order of kernel G_{rs}, whereas $\mathbb{K}_{rs}$ is a third order matrix, whose third dimension is equal to 2.

2.4. Major result of the paper

In what follows, analytical integrations will be carried out with reference to integral (21), but tables will be presented only for $\mathbb{K}_{rs}(\mathbf{x})$ for paucity of space. In such a case, it turns out that in the local coordinate system $\mathscr{L}$

$$\mathbb{K}_{rs}(\mathbf{x}) = \kappa \widehat{\mathbb{K}}_{rs}(\mathbf{x}, d_2, d_3) \Big|_{d_3 = ad_2 + k_a}^{d_3 = bd_2 + k_b} \Big|_{d_2 = -x_2}^{d_2 = \bar{y}_2 - x_2} \tag{23}$$

$\kappa \in \mathbb{R}$ depends on material parameters of the problem under consideration. $\mathbb{K}_{rs}$ is defined by a sum of basic terms as follows:

$$\widehat{\mathbb{K}}_{rs}(\mathbf{x}, d_2, d_3) = \mathbb{L}^{rs} \log(\zeta_2 + r) + \mathbb{A}^{rs} \operatorname{arctanh} \frac{d_3}{r} + \mathbb{I}^{rs} I_{\triangle}^{r^{-3}}(\mathbf{x}, d_2, d_3) + \mathbb{R}^{rs} r + \mathbb{S}^{rs} \frac{1}{r} + \mathbb{H}^{rs} \frac{1}{r^3} \tag{24}$$

where

- $I_{\triangle}^{r^{-3}}(\mathbf{x}, d_2, d_3)$is the Lebesgue integral of r^{-3} over T_j. It has been discussed in great detail in [26] and will be shortly summarized in Section 4.2.
- $\mathbb{L}^{rs}$, $\mathbb{A}^{rs}$, $\mathbb{I}^{rs}$, $\mathbb{R}^{rs}$, $\mathbb{S}^{rs}$, $\mathbb{H}^{rs}$ are vectors (for scalar problems) or third-order tensors (for vector problems). Their expressions are collected in Appendix C for potential problems. Owing to paucity of space, expressions for linear elasticity have not been included here and will appear in a separate report.

$\mathbb{K}_{rs}(\mathbf{x})$ depends on the kernel G_{rs}, on the selected element T_j and on the position of point $\mathbf{x}$. Weakly singular kernel $G_{uu}(\mathbf{d})$, strongly singular kernels $G_{up}(\mathbf{d}, \mathbf{l}(\mathbf{y}))$ and $G_{pu}(\mathbf{d}, \mathbf{n}(\mathbf{x}))$, and hyper-singular kernel $G_{pp}(\mathbf{d}, \mathbf{n}(\mathbf{x}), \mathbf{l}(\mathbf{y}))$ are *singular with respect to* $\mathbf{y}$ depending on the position of $\mathbf{x}$ with respect to T_j. The item $\mathbf{x} \notin \overline{T_j}$ (that, for all kernels, leads to a Lebesgue inner integral) and the item $\mathbf{x} \in T_j$ (that leads to an improper integral for G_{uu}, to a Cauchy's Principal Value (from now on shortened as CPV) for G_{up} and G_{pu}, and to a HFP for G_{pp}) will be therefore separately dealt with.

DOI: 10.1002/nme

Formulae (23, 24) will be derived in the next section and particularized to the single layer potential (Equations (43, 44)), to the double layer potential and its adjoint (Equations (50)–(52)), and to the hypersingular integral operator (Equations (60), (61)). This derivation requires a certain amount of details. The reader who does not feel interested in them may jump to Section 4 where formulae (23, 24) will be discussed.

3. ANALYTICAL INTEGRATIONS

Green's functions G_{uu}, G_{up}, G_{pu} and G_{pp} contain terms (3). Once they are placed into ${F_{rs}}_j^n(\mathbf{x})$, the following basic integrals must be dealt with:

$$\int_{ad_2+k_a}^{bd_2+k_b} \frac{d_3^k}{r^{2m+1}}\,\mathrm{d}d_3, \quad k,m\in\mathbb{N}_0$$

Identity

$$\frac{x^{2k}}{\alpha^2+x^2}=(-1)^k\frac{\alpha^{2k}}{\alpha^2+x^2}+\sum_{j=1}^{k}\binom{k}{j}(-1)^{k-j}(\alpha^2+x^2)^{j-1}(\alpha^2)^{k-j} \tag{25}$$

which comes out from the binomial expansion rule, permits to obtain the following recursive relationship that seems to be useful for analytical integrations:

$$\frac{d_3^k}{r^{2m+1}}=(-\alpha^2)^{\widehat{k}}\frac{d_3^{k_{[2]}}}{r^{2m+1}}+\sum_{j=1}^{\widehat{k}}\binom{\widehat{k}}{j}(-1)^{\widehat{k}-j}\sum_{h=0}^{j-1}\binom{j-1}{h}\alpha^{2(\widehat{k}-1-h)}\frac{d_3^{2h+k_{[2]}}}{r^{2m-1}}, \quad k,m\in\mathbb{N}_0 \tag{26}$$

where $\alpha^2=d_1^2+d_2^2$ is the squared projection of the distance on the plane $d_3=0$. Here and in the remainder of the section, the following notation will be considered:
$\widehat{k}=k\div 2$ division in $\mathbb{N}$.
$k_{[2]}=k-2\widehat{k}$ remainder of $k\div 2$ in $\mathbb{N}$.

3.1. Lebesgue integrals

Consider $\mathbf{x}\notin\overline{T_j}$, which implies $r\neq 0$ and the Lebesgue nature of integral (21). Exploiting recursively identity (26), the first contribution of ${F_{rs}}_j^n(\mathbf{x})$, namely

$$\int_{ad_2+k_a}^{bd_2+k_b} G_{rs}(\mathbf{d})\mathbf{d}_3^{\mathsf{T}}\,\mathrm{d}d_3$$

is reduced to the sum of a set of basic integrals; the following identities, which can be easily proved by induction, are required for most kernels:

$$\int\frac{x^j}{\sqrt{\alpha^2+x^2}}\,\mathrm{d}x=\mu(j)\alpha^j\log(x+\sqrt{\alpha^2+x^2})+\sum_{k=0}^{\widetilde{j}-1}\eta(k,j)\alpha^{2(\widetilde{j}-k-1)}x^{2k+1-j_{[2]}}\sqrt{\alpha^2+x^2} \tag{27}$$

$$\int\frac{x^{n_{[2]}}}{(\alpha^2+x^2)\sqrt{\alpha^2+x^2}}\,\mathrm{d}x=\frac{x-(\alpha^2+x)(n_{[2]})}{\alpha^2\sqrt{\alpha^2+x^2}} \tag{28}$$

DOI: 10.1002/nme

$$\int \frac{x^{n_{[2]}}}{(\alpha^2+x^2)^2\sqrt{\alpha^2+x^2}}\,\mathrm{d}x = \frac{3\,\alpha^2 x+2\,x^3-(\alpha^4+3\,\alpha^2 x+2\,x^3)\,n_{[2]}}{3\,\alpha^4\,(\alpha^2+x^2)^{3/2}} \tag{29}$$

$$\int \frac{x^{n_{[2]}}}{(\alpha^2+x^2)^3\sqrt{\alpha^2+x^2}}\,\mathrm{d}x = \frac{(15\,\alpha^4 x+20\,\alpha^2 x^3+8\,x^5)\,(1-n_{[2]})-3\,\alpha^6 n_{[2]}}{15\,\alpha^6\,(\alpha^2+x^2)^{5/2}} \tag{30}$$

where

$\widehat{j} = j \div 2$ division in $\mathbb{N}$.

$j_{[2]} = j - 2\widehat{j}$ remainder of $j \div 2$ in $\mathbb{N}$.

$\widetilde{j} = j - \widehat{j}$ complementary part of $j \div 2$ in $\mathbb{N}$.

$\mu(j) = (1-j_{[2]})(-1)^{\widehat{j}}\frac{j!}{(\widehat{j}!2^{\widehat{j}})^2}$

$\eta(k,j) = (-1)^{k-1-\widetilde{j}}\left((1-j_{[2]})\frac{j!}{(2k+1)!}\left(\frac{k!}{\widehat{j}!2^{\widehat{j}-k}}\right)^2 + j_{[2]}\frac{(2k)!}{j!}\left(\frac{\widehat{j-1}!}{k!2^{k-\widehat{j-1}}}\right)^2\right)$

In view of (27)–(30), it follows:

$$\int_{ad_2+k_a}^{bd_2+k_b} G_{rs}(\mathbf{d})\,\mathrm{d}_3^k\,\mathrm{d}d_3 = \sum_{l,m=0}^{3}\sum_{j=0}^{N(k,l,m)} \frac{\mathbf{A}_{lm}^j(\mathbf{x})}{(d_1^2+d_2^2)^l}\frac{d_2^j}{r^{2m-1}} + \sum_{j=0}^{k}\mathbf{B}^j(\mathbf{x})\,\mathrm{d}_2^j \log(d_3+r)\Bigg|_{d_3=ad_2+k_a}^{d_3=bd_2+k_b} \tag{31}$$

For scalar problems $\mathbf{A}_{lm}^j$ and $\mathbf{B}^j$ are scalar functions, whereas for vector problems they are matrices' functions of the same order (here termed N_{rs}: for elasticity,$N_{rs}=3$) of kernel G_{rs}. Of course, $\mathbf{A}_{lm}^j$ and $\mathbf{B}^j$ depend upon the considered kernel. Integral (31) can be recast in the vector formalism of Equation (21), namely

$$\int_{ad_2+k_a}^{bd_2+k_b} G_{rs}(\mathbf{d})\mathbf{d}_3^{\mathsf{T}}\,\mathrm{d}d_3 = \sum_{l,m=0}^{3}\frac{\widetilde{\mathbf{d}}_2^{\,\mathsf{T}}\mathbb{A}_{lm}(\mathbf{x})}{(d_1^2+d_2^2)^l r^{2m-1}} + \widetilde{\widetilde{\mathbf{d}}}_2^{\,\mathsf{T}}\mathbb{B}(\mathbf{x})\log(d_3+r)\Bigg|_{d_3=ad_2+k_a}^{d_3=bd_2+k_b} \tag{32}$$

Vectors $\widetilde{\mathbf{d}}_2$ and $\widetilde{\widetilde{\mathbf{d}}}_2$ are special instances of $\mathbf{d}_2$, with different cardinality, here termed as $\widetilde{N}_2$ and $\widetilde{\widetilde{N}}_2$, respectively; the latter is equal to the cardinality of $\mathbf{d}_3$, here termed as N_3; $\widetilde{N}_2$ depends also upon l and m. For scalar problems $\mathbb{A}_{lm}$ is a matrix $\widetilde{N}_2 \times N_3$ of functions, whereas for vector problems $\mathbb{A}_{lm}$ is a fourth-order matrix $\widetilde{N}_2 \times (N_{rs}\times N_{rs}) \times N_3$; analogously, for scalar problems $\mathbb{B}$ is a matrix $\widetilde{\widetilde{N}}_2 \times N_3$ of functions, whereas for vector problems $\mathbb{B}$ is a fourth-order matrix $\widetilde{\widetilde{N}}_2 \times (N_{rs}\times N_{rs}) \times N_3$.

Substituting expression (32) into ${F_{rs}}_j^n(\mathbf{x})$, it becomes

$${F_{rs}}_j^n(\mathbf{x}) = \sum_{l,m=0}^{3}\int_{-x_2}^{\bar{y}_2-x_2}\frac{\widetilde{\mathbf{d}}_2^{\,\mathsf{T}}\mathbb{A}_{lm}\mathbf{X}^{(3)\mathsf{T}}\Lambda_j^n\mathbf{X}^{(2)}\mathbf{d}_2}{(d_1^2+d_2^2)^l r^{2m-1}}\Bigg|_{d_3=ad_2+k_a}^{d_3=bd_2+k_b}\mathrm{d}d_2$$

$$+\int_{-x_2}^{\bar{y}_2-x_2}\widetilde{\widetilde{\mathbf{d}}}_2^{\,\mathsf{T}}\mathbb{B}\mathbf{X}^{(3)\mathsf{T}}\Lambda_j^n\mathbf{X}^{(2)}\mathbf{d}_2\log(d_3+r)\Bigg|_{d_3=ad_2+k_a}^{d_3=bd_2+k_b}\mathrm{d}d_2$$

DOI: 10.1002/nme

$$= \sum_{l,m=0}^{3} \int_{-x_2}^{\bar{y}_2-x_2} \frac{\widetilde{\mathbf{d}}_2^{\mathsf{T}} \mathbb{C}_{lm}{}_j^n \mathbf{d}_2}{(d_1^2+d_2^2)^l r^{2m-1}} \Bigg|_{d_3=ad_2+k_a}^{d_3=bd_2+k_b} \mathrm{d}d_2$$

$$+ \int_{-x_2}^{\bar{y}_2-x_2} \widetilde{\widetilde{\mathbf{d}}}_2^{\mathsf{T}} \mathbb{D}_j^n \mathbf{d}_2 \log(d_3+r) \Bigg|_{d_3=ad_2+k_a}^{d_3=bd_2+k_b} \mathrm{d}d_2 \tag{33}$$

with $\mathbb{C}_{lm}{}_j^n$ and $\mathbb{D}_j^n$ defined by comparison. To completely solve (21), only integrals

$$\int_{-x_2}^{\bar{y}_2-x_2} \frac{1}{(d_1^2+d_2^2)^l} \frac{d_2^h}{r^{2m-1}} \Bigg|_{d_3=ad_2+k_a}^{d_3=bd_2+k_b} \mathrm{d}d_2, \quad l,m=0,1,2,3, \quad h \in \mathbb{N}_0 \tag{34}$$

$$\int_{-x_2}^{\bar{y}_2-x_2} d_2^h \log(d_3+r) \Bigg|_{d_3=ad_2+k_a}^{d_3=bd_2+k_b} \mathrm{d}d_2, \quad h \in \mathbb{N}_0 \tag{35}$$

are required.

3.1.1. Single layer operator. Matrices $\mathbb{C}_{lm}{}_j^n$ vanish for $l,m=2,3$. Only the following integrals are of interest for the single layer potential:

$$\int_{-x_2}^{\bar{y}_2-x_2} \frac{d_2^k}{r} \Bigg|_{d_3=ad_2+k_a}^{d_3=bd_2+k_b} \mathrm{d}d_2 \tag{36}$$

$$\int_{-x_2}^{\bar{y}_2-x_2} \frac{d_2^k}{x_1^2+d_2^2} \frac{1}{r} \Bigg|_{d_3=ad_2+k_a}^{d_3=bd_2+k_b} \mathrm{d}d_2 \tag{37}$$

$$\int_{-x_2}^{\bar{y}_2-x_2} d_2^k \log(d_3+r) \Bigg|_{d_3=ad_2+k_a}^{d_3=bd_2+k_b} \mathrm{d}d_2 \tag{38}$$

Making use of the affine transformation

$$\zeta_2 = \frac{d_2+b\,\mathrm{d}_3}{\sqrt{1+b^2}} \Bigg|^{d_3=bd_2+k_b} \tag{39}$$

integral (36) becomes

$$\sum_{j=0}^{k} \binom{k}{j} \frac{(-bk_b)^{k-j}}{(\sqrt{1+b^2})^{2k+1-j}} \int_{bk_b/(\sqrt{1+b^2})-\sqrt{1+b^2}x_2}^{bk_b/(\sqrt{1+b^2})+\sqrt{1+b^2}(\bar{y}_2-x_2)} \frac{\zeta_2^j}{\sqrt{d_1^2+\dfrac{k_b^2}{1+b^2}+\zeta_2^2}} \mathrm{d}\zeta_2 \tag{40}$$

which has a closed form owing to outcome (27). By defining with $\gamma: \mathbb{N}\times\mathbb{N}\times\mathbb{N}_0\times\mathbb{R}\to\mathbb{R}$ the function

$$\gamma(k,j,h,d_1) \stackrel{\text{def}}{=} \binom{\widehat{k}}{j} \binom{j-1}{h} (-1)^{\widehat{k}-j} (d_1^2)^{\widehat{k}-1-h} \tag{41}$$

DOI: 10.1002/nme

and by means of identity (25), Equation (37) will be rewritten as

$$(-1)^{\widehat{k}} d_1^{2\widehat{k}} \int_{-x_2}^{\bar{y}_2-x_2} \frac{d_2^{k_{[2]}}}{(x_1^2+d_2^2)} \frac{1}{r} \Bigg|_{d_3=ad_2+k_a}^{d_3=bd_2+k_b} \mathrm{d}d_2 + \sum_{j=1}^{\widehat{k}} \sum_{h=0}^{j-1} \gamma(k,j,h,d_1)$$

$$\times \int_{-x_2}^{\bar{y}_2-x_2} \frac{d_2^{k_{[2]}+2h}}{r} \Bigg|_{d_3=ad_2+k_a}^{d_3=bd_2+k_b} \mathrm{d}d_2 \tag{42}$$

Integral (42) has a closed form in view of (40), (A2) of Appendix B. Finally, the closed form of integral (38) is given in Appendix B by Equation (A6).

Algebraic manipulations lead from (40), (42) and (A6) to the following tabular expression:

$$\mathbb{K}_{uu}(\mathbf{x}) = \kappa \widehat{\mathbb{K}}_{uu}(\mathbf{x}, d_2, \vartheta d_2 + k_\vartheta)|_{\vartheta=a}^{\vartheta=b} \Big|_{d_2=-x_2}^{d_2=\bar{y}_2-x_2} \tag{43}$$

with

$$\widehat{\mathbb{K}}_{uu}(\mathbf{x}, d_2, d_3) = \mathbb{L}^{uu} \log(\zeta_2 + r) + \mathbb{A}^{uu} \operatorname{arctanh} \frac{d_3}{r} + \mathbb{I}^{uu} I_{\triangle}^{r^{-3}}(\mathbf{x}, d_2, d_3) + \mathbb{R}^{uu} r \tag{44}$$

For potential problems, $\kappa = (4\alpha\pi)^{-1}$ whereas for linear elasticity, $\kappa = (16G(1-\nu)\pi)^{-1}$ Outcome (43) can straightforwardly be extended to polynomial shape functions of arbitrarily degree over flat triangles accordingly to (33).

3.1.2. Double layer operator. Besides (36)–(38), one has to deal with the following integrals:

$$\int_{-x_2}^{\bar{y}_2-x_2} \frac{d_2^k}{(x_1^2+d_2^2)^2} \frac{1}{r} \Bigg|_{d_3=ad_2+k_a}^{d_3=bd_2+k_b} \mathrm{d}d_2 \tag{45}$$

$$\int_{-x_2}^{\bar{y}_2-x_2} \frac{d_2^k}{r^{3/2}} \Bigg|_{d_3=ad_2+k_a}^{d_3=bd_2+k_b} \mathrm{d}d_2 \tag{46}$$

$$\int_{-x_2}^{\bar{y}_2-x_2} \frac{d_2^k}{(x_1^2+d_2^2)} \frac{1}{r^{3/2}} \Bigg|_{d_3=ad_2+k_a}^{d_3=bd_2+k_b} \mathrm{d}d_2 \tag{47}$$

By means of identities (25) and (41), integral (45) can be rewritten as

$$(-1)^{\widehat{k}} d_1^{2\widehat{k}} \int_{-x_2}^{\bar{y}_2-x_2} \frac{d_2^{k_{[2]}}}{(x_1^2+d_2^2)^2} \frac{1}{r} \Bigg|_{d_3=ad_2+k_a}^{d_3=bd_2+k_b} \mathrm{d}d_2$$

$$+ \sum_{j=1}^{\widehat{k}} \sum_{h=0}^{j-1} \gamma(k,j,h,d_1) \int_{-x_2}^{\bar{y}_2-x_2} \frac{d_2^{k_{[2]}+2h}}{(x_1^2+d_2^2)} \frac{1}{r} \Bigg|_{d_3=ad_2+k_a}^{d_3=bd_2+k_b} \mathrm{d}d_2 \tag{48}$$

DOI: 10.1002/nme

Integral (48) has a closed form in view of (A3) of Appendix B. Making use of affine transformation (39), integral (46) becomes

$$\sum_{j=0}^{k}\binom{k}{j}\frac{(-bk_b)^{k-j}}{(\sqrt{1+b^2})^{2k+1-j}}\int_{(bk_b)/\sqrt{1+b^2}-\sqrt{1+b^2}x_2}^{(bk_b)/\sqrt{1+b^2}+\sqrt{1+b^2}(\bar{y_2}-x_2)}\frac{\zeta_2^j}{\left(d_1^2+\dfrac{k_b^2}{1+b^2}+\zeta_2^2\right)^{3/2}}\,\mathrm{d}\zeta_2 \tag{49}$$

which has a closed form in view of (25), (27), (28). Finally, following the same path of reasoning used for integral (37), one obtains the closed form of (47) in view of (49, A8) of Appendix B.

Algebraic manipulations lead to

$$\mathbb{K}_{up}(\mathbf{x})=\kappa\widehat{\mathbb{K}}_{up}(\mathbf{x},d_2,\vartheta d_2+k_\vartheta)|_{\vartheta=a}^{\vartheta=b}\Big|_{d_2=-x_2}^{d_2=\bar{y_2}-x_2},\qquad \mathbb{K}_{pu}(\mathbf{x})=\kappa\widehat{\mathbb{K}}_{pu}(\mathbf{x},d_2,\vartheta d_2+k_\vartheta)|_{\vartheta=a}^{\vartheta=b}\Big|_{d_2=-x_2}^{d_2=\bar{y_2}-x_2} \tag{50}$$

with

$$\widehat{\mathbb{K}}_{up}(\mathbf{x},d_2,d_3)=\mathbb{L}^{up}\log(\zeta_2+r)+\mathbb{A}^{up}\operatorname{arctanh}\frac{d_3}{r}+\mathbb{I}^{up}I_{\triangle}^{r^{-3}}(\mathbf{x},d_2,d_3)+\mathbb{R}^{up}r+\mathbb{S}^{up}\frac{1}{r} \tag{51}$$

$$\widehat{\mathbb{K}}_{pu}(\mathbf{x},d_2,d_3)=\mathbb{L}^{pu}\log(\zeta_2+r)+\mathbb{A}^{pu}\operatorname{arctanh}\frac{d_3}{r}+\mathbb{I}^{pu}I_{\triangle}^{r^{-3}}(\mathbf{x},d_2,d_3)+\mathbb{R}^{pu}r+\mathbb{S}^{pu}\frac{1}{r} \tag{52}$$

For potential problems, $\kappa=1/(4\pi)$ whereas for linear elasticity, $\kappa=1/(8\pi(1-\nu))$. Identities (50), which hold for linear shape functions in view of Equation (22), can straightforwardly be extended to polynomial shape functions of arbitrarily degree over flat triangles accordingly to (33).

3.1.3. Derivative of the double layer operator. The evaluation of integrals (36)–(38) and (45)–(47) is required. Moreover

$$\int_{-x_2}^{\bar{y_2}-x_2}\frac{d_2^k}{(x_1^2+d_2^2)^3}\frac{1}{r}\Big|_{d_3=ad_2+k_a}^{d_3=bd_2+k_b}\mathrm{d}d_2 \tag{53}$$

$$\int_{-x_2}^{\bar{y_2}-x_2}\frac{d_2^k}{(x_1^2+d_2^2)^2}\frac{1}{r^{3/2}}\Big|_{d_3=ad_2+k_a}^{d_3=bd_2+k_b}\mathrm{d}d_2 \tag{54}$$

$$\int_{-x_2}^{\bar{y_2}-x_2}\frac{d_2^k}{r^{5/2}}\Big|_{d_3=ad_2+k_a}^{d_3=bd_2+k_b}\mathrm{d}d_2 \tag{55}$$

$$\int_{-x_2}^{\bar{y_2}-x_2}\frac{d_2^k}{(x_1^2+d_2^2)}\frac{1}{r^{5/2}}\Big|_{d_3=ad_2+k_a}^{d_3=bd_2+k_b}\mathrm{d}d_2 \tag{56}$$

DOI: 10.1002/nme

have to be faced. The path of reasoning used for solving integral (45) applies to (53) and (54) as well. They will be rewritten as

$$(-1)^{\widehat{k}} d_1^{2\widehat{k}} \int_{-x_2}^{\bar{y}_2-x_2} \frac{d_2^{k_{[2]}}}{(x_1^2+d_2^2)^3} \frac{1}{r} \Bigg|_{d_3=ad_2+k_a}^{d_3=bd_2+k_b} \mathrm{d}d_2 + \sum_{j=1}^{\widehat{k}} \sum_{h=0}^{j-1} \gamma(k,j,h,d_1) \int_{-x_2}^{\bar{y}_2-x_2} \frac{d_2^{k_{[2]}+2h}}{(x_1^2+d_2^2)^2} \frac{1}{r} \Bigg|_{d_3=ad_2+k_a}^{d_3=bd_2+k_b} \mathrm{d}d_2 \tag{57}$$

and

$$(-1)^{\widehat{k}} d_1^{2\widehat{k}} \int_{-x_2}^{\bar{y}_2-x_2} \frac{d_2^{k_{[2]}}}{(x_1^2+d_2^2)^2} \frac{1}{r^{3/2}} \Bigg|_{d_3=ad_2+k_a}^{d_3=bd_2+k_b} \mathrm{d}d_2 + \sum_{j=1}^{\widehat{k}} \sum_{h=0}^{j-1} \gamma(k,j,h,d_1) \int_{-x_2}^{\bar{y}_2-x_2} \frac{d_2^{k_{[2]}+2h}}{(x_1^2+d_2^2)} \frac{1}{r^{3/2}} \Bigg|_{d_3=ad_2+k_a}^{d_3=bd_2+k_b} \mathrm{d}d_2 \tag{58}$$

respectively. Integrals (57)–(58) have closed forms in view of (A4), (A9) of Appendix B. By means of affine transformation (39), integral (55) becomes

$$\sum_{j=0}^{k} \binom{k}{j} \frac{(-bk_b)^{k-j}}{(\sqrt{1+b^2})^{2k+1-j}} \int_{(bk_b)/\sqrt{1+b^2}-\sqrt{1+b^2}x_2}^{(bk_b)/\sqrt{1+b^2}+\sqrt{1+b^2}(\bar{y}_2-x_2)} \left(\frac{1}{d_1^2+\dfrac{k_b^2}{1+b^2}+\zeta_2^2} \right)^2 \frac{\zeta_2^j}{\sqrt{d_1^2+\dfrac{k_b^2}{1+b^2}+\zeta_2^2}} \mathrm{d}\zeta_2 \tag{59}$$

which has a closed form in view of (25), (27)–(29). Finally, following the same path of reasoning used for equation (37), the closed form of (56) comes out in view of (58) and of (A10) of Appendix B.

Algebraic manipulations lead to

$$\mathbb{K}_{pp}(\mathbf{x}) = \kappa \widehat{\mathbb{K}}_{pp}(\mathbf{x}, d_2, d_3) \Big|_{\vartheta=a}^{\vartheta=b} \Big|_{d_2=-x_2}^{d_2=\bar{y}_2-x_2} \tag{60}$$

with

$$\widehat{\mathbb{K}}_{pp}(\mathbf{x}, d_2, d_3) = \mathbb{L}^{pp} \log(\zeta_2+r) + \mathbb{A}^{pp} \operatorname{arctanh} \frac{d_3}{r} + \mathbb{I}^{pp} I_{\triangle}^{r^{-3}}(\mathbf{x}, d_2, d_3) + \mathbb{R}^{pp} r + \mathbb{S}^{pp} \frac{1}{r} + \mathbb{H}^{pp} \frac{1}{r^3} \tag{61}$$

For potential problems, $\kappa = \alpha/(4\pi)$, whereas for linear elasticity, $\kappa = G/(4\pi(1-\nu))$.

3.2. Singular integrals

3.2.1. HFP. Provided that regularity requirements are satisfied, peculiarities of Green's functions allow to perceive hypersingular integral (21) as a HFP in the limit process $\Omega \ni \mathbf{x} \to \mathbf{x} \in \Gamma$

DOI: 10.1002/nme

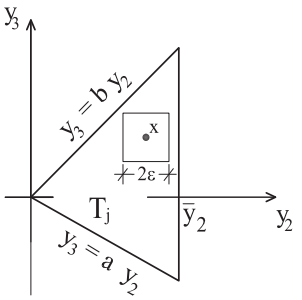

Figure 3. Geometrical description of a square neighborhood.

[27, 8, 28–30]. The definition of the finite part can be given as follows:

Definition 1
Let $\varepsilon \to I(\varepsilon)$ denote a complex-valued function that is continuous in $(0, \varepsilon_0)$ and assume that

$$I(\varepsilon) = I_0 + I_1 \log(\varepsilon) + \sum_{j=2}^{m} I_j \varepsilon^{1-j} + o(1), \quad \varepsilon \to 0$$

where $I_j \in \mathbb{C}$. Then I_0 is called the finite part of $I(\varepsilon)$. In dealing with the integrals, the finite part I_0 of a (usually) divergent integral $\int_{-\infty}^{+\infty} \phi(t)\,\mathrm{d}t$ is denoted by the symbol $\text{⨍}_{-\infty}^{+\infty} \phi(t)\,\mathrm{d}t$.

Definition 2
Assume that $\mathbf{x} \notin \partial T_j$ and define with

$$T_j^{\varepsilon} = \{\mathbf{y} \in T_j : |y_2 - x_2| < \varepsilon \text{ and } |y_3 - x_3| < \varepsilon\}$$

the domain in Figure 3. In agreement with Equation (22), define with

$$I_{\square}(\mathbf{x}, \varepsilon) \stackrel{\text{def}}{=} \int_{T_j \setminus T_j^{\varepsilon}} G_{pp}(\mathbf{d}; \mathbf{e}_1; \mathbf{e}_1)\,\mathrm{d}d_3\,\mathrm{d}d_2$$

Consider first $\mathbf{x} \in T_j$. Elastostatic kernel G_{pp} and potential kernel G_{pp}^{lapl} simplify as

$$G_{pp}(\mathbf{d}; \mathbf{e}_1; \mathbf{e}_1) = \frac{Gv}{(1-v)} \left\{ 2(\mathbf{e}_1 \otimes \mathbf{e}_1) + \frac{(1-2v)}{v}\mathbf{I} + 3\frac{\mathbf{d} \otimes \mathbf{d}}{r^2} \right\} \frac{1}{4\pi r^3}, \quad G_{pp}^{lapl}(\mathbf{d}; \mathbf{e}_1; \mathbf{e}_1) = -\frac{\alpha}{4\pi r^3}$$

in local coordinate system $\mathscr{L}$. With reference to elastostatic kernel G_{pp}, by direct integration

$$I_{\square}(\mathbf{x}, \varepsilon) = \frac{2\kappa}{k_{\vartheta}} \left\{ \frac{v}{r} \begin{pmatrix} 0 & 0 & 0 \\ 0 & d_2 & d_3 \\ 0 & d_3 & -d_2 \end{pmatrix} - \frac{r}{d_2} \begin{pmatrix} 1 & 0 & 0 \\ 0 & 1 & 0 \\ 0 & 0 & 1-v \end{pmatrix} \right\} \Bigg|_{d_3 = a d_2 + k_a, \vartheta = a}^{d_3 = b d_2 + k_b, \vartheta = b} \Bigg|_{d_2 = -x_2}^{d_2 = \bar{y}_2 - x_2}$$

$$+ I_2 \frac{1}{\varepsilon} + o(1), \quad \varepsilon \to 0 \tag{62}$$

DOI: 10.1002/nme

where

$$\kappa=\frac{G}{8\pi(1-\nu)},\quad I_2=4\kappa\sqrt{2}\begin{pmatrix}2&0&0\\0&2-\nu&0\\0&0&2-\nu\end{pmatrix} \tag{63}$$

The finite part immediately follows from its definition. The same result follows from a limit process, by taking $d_1\to 0^+$ in Equations (60, 61). Considering only the term pertaining to a constant shape function, it holds in fact

$$\lim_{d_1\to 0^+}\mathbb{L}^{pp}=\lim_{d_1\to 0^+}\mathbb{A}^{pp}=\lim_{d_1\to 0^+}\mathbb{I}^{pp}=\lim_{d_1\to 0^+}\mathbb{H}_{pp}=0$$

$$\lim_{d_1\to 0^+}\mathbb{R}_{pp}=-\frac{2}{d_2k_\vartheta}\begin{pmatrix}1&0&0\\0&1&0\\0&0&1-\nu\end{pmatrix}$$

$$\lim_{d_1\to 0^+}\mathbb{S}_{pp}=\frac{2\nu}{k_\vartheta}\begin{pmatrix}0&0&0\\0&d_2&d_3\\0&d_3&-d_2\end{pmatrix}$$

With the same path of reasoning, by direct integration it follows for the potential kernel G_{pp}^{lapl}:

$$I_\square^{lapl}(\mathbf{x},\varepsilon)=\frac{\kappa}{k_\vartheta}\frac{r}{d_2}\Big|_{d_3=ad_2+k_a,\vartheta=a}^{d_3=bd_2+k_b,\vartheta=b}\Big|_{d_2=-x_2}^{d_2=\bar{y}_2-x_2}+\frac{4\kappa\sqrt{2}}{\varepsilon}+o(1),\quad \varepsilon\to 0 \tag{64}$$

and the finite part immediately follows from its definition. The same result follows from a limit process, by taking $d_1\to 0^+$ in Equations (60, 61). It holds in fact

$$\lim_{d_1\to 0^+}\mathbb{L}^{qq}=\lim_{d_1\to 0^+}\mathbb{A}^{qq}=\lim_{d_1\to 0^+}\mathbb{I}^{qq}=\lim_{d_1\to 0^+}\mathbb{S}_{qq}=\lim_{d_1\to 0^+}\mathbb{H}_{qq}=0$$

$$\lim_{d_1\to 0^+}\mathbb{R}_{qq}=\frac{1}{d_2k_\vartheta}$$

3.2.2. Cauchy's principal value. Considerations about the nature of the singularity in the boundary limit apply to the CPV as well. Consider first the point $\mathbf{x}\in\Gamma$, so that kernel G_{pu} in the local coordinate system $\mathscr{L}$ simplifies as

$$G_{pu}(\mathbf{d};\mathbf{e}_1)=\frac{1}{4\pi}\frac{(1-2\nu)}{(1-\nu)}\frac{1}{r^3}\mathbf{SKW}(\mathbf{d}\otimes\mathbf{e}_1)$$

By direct integration

$$\int_{T_j\setminus T_j^\varepsilon}G_{pu}(\mathbf{d};\mathbf{e}_1)\,\mathrm{d}\Gamma=2\kappa\left[\alpha\,\mathrm{arctanh}\frac{d_3}{r}-\frac{\beta}{\sqrt{1+\vartheta^2}}\log(\zeta_2+r)\right]\Big|_{\substack{d_3=ad_2+k_a\\ \vartheta=a}}^{\substack{d_3=bd_2+k_b\\ \vartheta=b}}\Big|_{d_2=-x_2}^{d_2=\bar{y}_2-x_2}+o(1),\ \varepsilon\to 0 \tag{65}$$

DOI: 10.1002/nme

where

$$\kappa=\frac{1-2v}{8\pi(1-v)},\quad \alpha=\mathbf{SKW}(\mathbf{e}_1\otimes\mathbf{e}_2),\quad \beta=\vartheta\alpha-\mathbf{SKW}(\mathbf{e}_1\otimes\mathbf{e}_3)$$

which is the CPV by definition. Identity (65) follows even through a limit process, by taking $d_1\to 0^+$ in (52). Considering only the terms pertaining to a constant shape function, it holds in fact

$$\lim_{d_1\to 0^+}\mathbb{L}^{pu}=\begin{pmatrix}0 & -B & 1\\ b & 0 & 0\\ -1 & 0 & 0\end{pmatrix}\frac{1-2v}{\sqrt{1+b^2}}$$

$$\lim_{d_1\to 0^+}\mathbb{A}^{pu}=2(1-2v)\mathbf{SKW}(\mathbf{e}_1\otimes\mathbf{e}_2)$$

$$\lim_{d_1\to 0^+}\mathbb{R}^{pu}=\lim_{d_1\to 0^+}\mathbb{S}^{pu}=0$$

Strongly singular kernels G_{up} and G_{pu} generate free-terms [13] that holds $\frac{1}{2}\mathbb{1}$ for smooth boundaries in the limit process $\Omega\ni\mathbf{x}\to\mathbf{x}\in\Gamma$. Such free-terms arise in the limit

$$\lim_{d_1\to 0^+}[\mathbb{I}^{pu}I_{\triangle}^{r^{-3}}(\mathbf{x},d_2,d_3)]_{d_3=ad_2+k_a}^{d_3=bd_2+k_b}\Big|_{d_2=-x_2}^{d_2=\bar{y}_2-x_2} \tag{66}$$

In fact, taking into account the expansion

$$\mathbb{I}^{pu}=2\,\mathrm{d}_1(1-v)\mathbb{1}+o(d_1),\quad d_1\to 0$$

it can be easily shown that

$$\kappa\lim_{d_1\to 0^+}[\mathbb{I}^{pu}I_{\triangle}^{r^{-3}}(\mathbf{x},d_2,d_3)]_{d_3=ad_2+k_a}^{d_3=bd_2+k_b}\Big|_{d_2=-x_2}^{d_2=\bar{y}_2-x_2}=\frac{1}{2}[1\quad 0] \tag{67}$$

By inserting outcome (67) into Equation (22), it follows that

$$\frac{1}{2}[1\quad 0]\begin{bmatrix}1-\dfrac{x_2}{\bar{y}_2}\\ \dfrac{1}{\bar{y}_2}\end{bmatrix}=\frac{1}{2}\varphi_j^n(\mathbf{x})$$

which is the discrete counterpart of the free-term for smooth boundaries.

4. DISCUSSION

4.1. Literature review

Analytical integrations have been basically performed toward three schemes. In the first scheme (see e.g. [14, 31]), the source point is fixed, whereas the boundary around the source point is temporarily deformed to allow an analytical evaluation of contributions from singular kernels; then

DOI: 10.1002/nme

the limit is taken as the deformed boundary shrinks back to the actual boundary. In the second approach, see among others [32–34], the source point $\mathbf{x}$ is first moved away from the boundary; integrals are evaluated analytically and a limit process is then performed to bring the source point back to the boundary. In all the aforementioned papers, analytical integrations are provided for all singular integrals, whereas standard quadrature formulae are used for non-singular integrals. In the third scheme [26, 35–37], the complete analytical integration has been provided, also in time-dependent problems [38], evaluating HFP and CPV directly as well as by means of a limit to the boundary process. The present note falls into this class.

4.2. *On function* $I_{\triangle}^{r^{-3}}(\mathbf{x})$ *and its implementation*

A preliminary work [26] concerned the analytical integration of function r^{-3} over triangle T_j, as the sum of two factors $I_{\triangle}^{r^{-3}}(\mathbf{x}, d_2)$:

$$I_{\triangle}^{r^{-3}}(\mathbf{x}) = \int_{-x_2}^{\bar{y}_2 - x_2} \int_{ad_2+k_a}^{bd_2+k_b} \frac{1}{r^3}\,\mathrm{d}d_3\,\mathrm{d}d_2 = I_{\triangle}^{r^{-3}}(\mathbf{x}, d_2)\Big|_{-x_2}^{\bar{y}_2 - x_2} \tag{68}$$

where $I_{\triangle}^{r^{-3}}(.,.) : \{\mathbb{R}^3 \backslash T_j \times [-x_2, \bar{y}_2 - x_2]\} \to \mathbb{R}$ was defined by

$$I_{\triangle}^{r^{-3}}(\mathbf{x}, d_2) = \int \mathrm{d}d_2 \int_{ad_2+k_a}^{bd_2+k_b} \frac{1}{r^3}\,\mathrm{d}d_3 = I_{\triangle}^{r^{-3}}(\mathbf{x}, d_2, d_3)\Big|_{d_3 = ad_2+k_a}^{d_3 = bd_2+k_b} \tag{69}$$

Focusing on the upper extremum $d_3 = bd_2 + k_b$, and defining with

$$\Upsilon(\mathbf{x}, d_2, bd_2+k_b) = bd_1 + \frac{b(d_1^2+d_2^2)d_1}{2d_2^2} + \frac{(d_1^2+d_2^2)((d_1^2+d_2^2)b^2+d_2^2)d_1}{2d_2^2(d_2k_b - bd_1^2)} + \frac{(d_1^2-d_2^2)k_b}{2d_2d_1}$$

two candidate functions for $I_{\triangle}^{r^{-3}}(\mathbf{x}, d_2, bd_2+k_b)$ arise, namely

$$f_1^b(\mathbf{x}, d_2, bd_2+k_b) = \frac{1}{2d_1} \arctan \frac{r}{\Upsilon(\mathbf{x}, d_2, bd_2+k_b)}$$

$$f_2^b(\mathbf{x}, d_2, bd_2+k_b) = -\frac{1}{2d_1} \arctan \frac{\Upsilon(\mathbf{x}, d_2, bd_2+k_b)}{r}$$

which are linked by

$$f_1^b - f_2^b = \frac{\pi}{4d_1} \mathrm{sgn} \frac{\Upsilon(\mathbf{x}, d_2, bd_2+k_b)}{r} \tag{70}$$

The (unique) function $I_{\triangle}^{r^{-3}}(\mathbf{x}, d_2, bd_2+k_b)$ can be caught in studying the domain in which f_1^b and f_2^b are defined. Within a domain where both f_1^b and f_2^b are defined, they have the same derivative, but they differ by a constant. Within a domain in which only f_1^b (or f_2^b) is everywhere defined, f_1^b (or f_2^b) is the unique primitive. The analysis is quite involved: a flow chart summarizes it in Figure 4.

DOI: 10.1002/nme

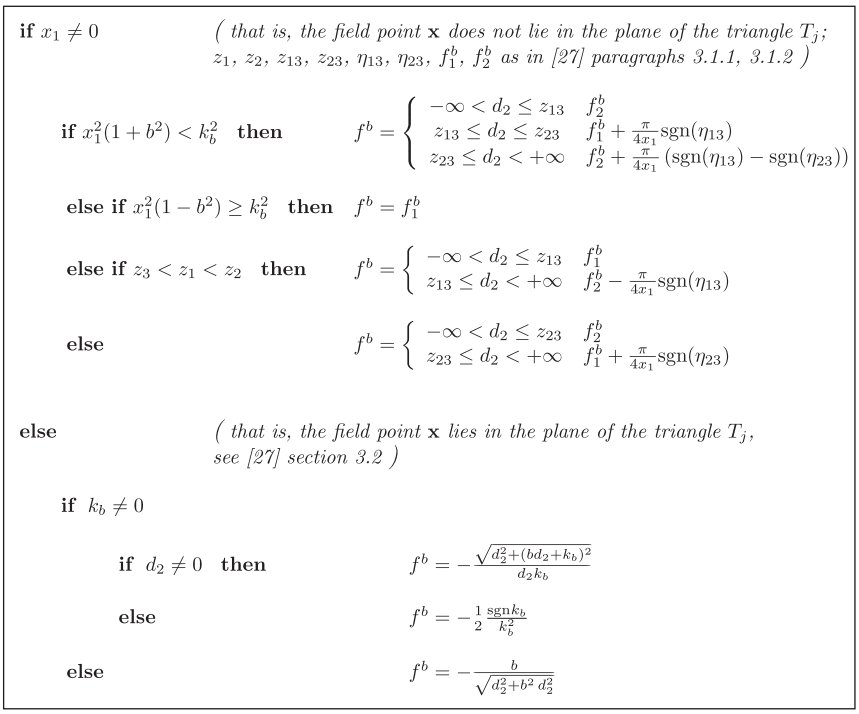

Figure 4. A flow chart of $f^b(\mathbf{x}, d_2)$.

4.3. Implementation details

The singularity analysis performed in Section 3.2 does not apply when $\mathbf{x} \in \partial T_j$: as it is well known, the limit to the boundary process looses any meaning, because a uniquely defined normal to the boundary cannot—in general—be identified on Γ when $\mathbf{x} \in \partial T_j$.

4.3.1. Evaluation of matrices $\mathbb{R}^{pp}$, $\mathbb{S}^{pp}$, $\mathbb{H}^{pp}$. The evaluation of matrices $\mathbb{R}^{pp}$, $\mathbb{S}^{pp}$, $\mathbb{H}^{pp}$ requires particular care when point $\mathbf{x}$ belongs to the lines that define the sides of T_j, even for $\mathbf{x} \notin \partial T_j$.

In view of definitions (A1) and (A7), in the analysis of matrices $\mathbb{R}^{pp}$, $\mathbb{S}^{pp}$ for potential problems three issues shall be investigated, namely: $\vartheta^2 \mathrm{d}_1^2 + k_\vartheta^2 = 0$, $(1+\vartheta^2)\mathrm{d}_1^2 + k_\vartheta^2 = 0$ and $d_1^2 + d_2^2 = 0$. Their meaning is summarized in Figure 5.

Item $\vartheta = k_\vartheta = 0$ is the most peculiar, because it identifies a whole plane, the $x_3 = 0$ one, in which neither $\mathbb{R}^{pp}$ nor $\mathbb{S}^{pp}$ is defined. The sum

$$\mathbb{R}^{pp} r + \mathbb{S}^{pp} \frac{1}{r}\Big|_{d_2=-x_2}^{d_2=\bar{y}_2-x_2} \cdot \mathbf{e}_1 = \begin{cases} -\dfrac{d_2 n_3}{d_1}\dfrac{1}{r}\Big|_{d_2=-x_2}^{d_2=\bar{y}_2-x_2}, & x_1 \neq 0 \\ 0, & x_1 = 0,\ x_2 < 0 \quad \text{or} \quad x_2 > \bar{y}_2. \end{cases} \tag{71}$$

DOI: 10.1002/nme

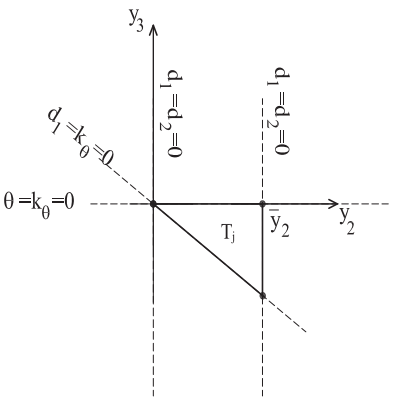

Figure 5. The three special cases $\vartheta^2 d_1^2 + k_\vartheta^2 = 0$, $(1+\vartheta^2)d_1^2 + k_\vartheta^2 = 0$ and $d_1^2 + d_2^2 = 0$ and their geometrical meaning.

is well defined however when $\mathbf{x} \notin \partial T_j$. Noting that $-d_2 n_3/d_1$ is the constant term of the expansion of $\mathbb{S}^{pp} \cdot \mathbf{e}_1$ about $\vartheta = 0$, algorithm (61) can be kept as it stands by assuming

$$\mathbb{S}^{pp} \cdot \mathbf{e}_1 = \begin{cases} \lambda(\vartheta)\Lambda(\vartheta) d_1 \mathbf{n} \cdot \boldsymbol{\alpha}, & \vartheta \neq 0 \quad \text{or} \quad k_\vartheta \neq 0 \\ \dfrac{d_2 n_3}{d_1}, & x_1 \neq 0 \\ 0, & x_1 = 0,\ x_2 < 0 \quad \text{or} \quad x_2 > \bar{y}_2 \end{cases}$$

$$\mathbb{R}^{pp} \cdot \mathbf{e}_1 = \begin{cases} \dfrac{\lambda(\vartheta)}{(d_1^2 + d_2^2)} \mathbf{n} \cdot \boldsymbol{\gamma}, & \vartheta \neq 0 \quad \text{or} \quad k_\vartheta \neq 0 \\ 0, & \text{otherwise} \end{cases}$$

Similar remarks apply to the linear term in algorithm (61) that can be kept as it stands by assuming

$$\mathbb{S}^{pp} \cdot \mathbf{e}_2 = \begin{cases} \lambda(\vartheta)\Lambda(\vartheta) d_1 \mathbf{n} \cdot \boldsymbol{\alpha}, & \vartheta \neq 0 \quad \text{or} \quad k_\vartheta \neq 0 \\ -d_1 n_3, & x_1 \neq 0 \\ 0, & x_1 = 0,\ x_2 < 0 \quad \text{or} \quad x_2 > \bar{y}_2. \end{cases}$$

$$\mathbb{R}^{pp} \cdot \mathbf{e}_2 = \begin{cases} \dfrac{\lambda(\vartheta)}{(d_1^2 + d_2^2)} \mathbf{n} \cdot \boldsymbol{\gamma}, & \vartheta \neq 0 \quad \text{or} \quad k_\vartheta \neq 0 \\ 0, & \text{otherwise} \end{cases}$$

Vectors $\boldsymbol{\alpha}$ and $\boldsymbol{\gamma}$ have been defined in Appendix C.

The two equalities $d_1 = k_\vartheta = 0$ identify two sides of T_j. Neither $\mathbb{R}^{pp}$ nor $\mathbb{S}^{pp}$ are defined, but the sum

$$\mathbb{R}^{pp} r + \mathbb{S}^{pp} \frac{1}{r}\bigg|_{d_2=-x_2}^{d_2=\bar{y}_2-x_2} \cdot \mathbf{e}_1 = \vartheta n_1 \frac{1}{r}\bigg|_{d_2=-x_2}^{d_2=\bar{y}_2-x_2}, \quad x_2 < 0 \quad \text{or} \quad x_2 > \bar{y}_2 \tag{72}$$

DOI: 10.1002/nme

is well defined, however when $\mathbf{x} \notin \partial T_j$. Algorithm (61) can be kept as it stands by assuming

$$\mathbb{S}^{pp} \cdot \mathbf{e}_1 = \begin{cases} \lambda(\vartheta)\Lambda(\vartheta) d_1 \mathbf{n} \cdot \boldsymbol{\alpha}, & d_1 \neq 0 \quad \text{or} \quad k_\vartheta \neq 0 \\ -\vartheta n_1, & x_2 < 0 \quad \text{or} \quad x_2 > \bar{y}_2 \end{cases}$$

$$\mathbb{R}^{pp} \cdot \mathbf{e}_1 = \begin{cases} \dfrac{\lambda(\vartheta)}{(d_1^2 + d_2^2)} \mathbf{n} \cdot \boldsymbol{\gamma}, & \vartheta \neq 0 \quad \text{or} \quad k_\vartheta \neq 0 \\ 0 & \text{otherwise} \end{cases}$$

The linear term does not require particular care.

The last case, $d_1 = d_2 = 0$, concerns the side of T_j orthogonal to plane $y_3 = 0$. Vector $\mathbb{S}^{pp}$ is well defined (it is vanishing indeed), whereas $\mathbb{R}^{pp}$ is not. The quantity

$$\mathbb{R}^{pp} r \Big|_{\vartheta=a}^{\vartheta=b} \cdot \mathbf{e}_1 = \frac{\vartheta n_1}{k_\vartheta^2} r \Bigg|_{\vartheta=a}^{\vartheta=b}, \qquad \frac{x_3}{\bar{y}_2} < a \quad \text{or} \quad \frac{x_3}{\bar{y}_2} > b \tag{73}$$

is well defined, however when $\mathbf{x} \notin \partial T_j$. Algorithm (61) can be kept as it stands by assuming

$$\mathbb{R}^{pp} \cdot \mathbf{e}_1 = \begin{cases} \dfrac{\lambda(\vartheta)}{(d_1^2 + d_2^2)} \mathbf{n} \cdot \boldsymbol{\gamma}, & d_1 \neq 0 \quad \text{or} \quad d_2 \neq 0 \\ \dfrac{\vartheta n_1}{k_\vartheta^2}, & \dfrac{x_3}{\bar{y}_2} < a \quad \text{or} \quad \dfrac{x_3}{\bar{y}_2} > b \end{cases}$$

The linear term does not require particular care.

4.3.2. Evaluation of $\operatorname{arctanh}(d_3/r)$. Function $\operatorname{arctanh}(d_3/r)$ is not defined when $|d_3/r| = 1$, that is when $d_1 = d_2 = 0$. This last condition defines the line of the side of T_j parallel to axis y_3 and its parallel through the center of the coordinate system (see Figure 5). It can be seen from Figure 6 that $\mathbf{x} \notin \partial T_j$ implies $\operatorname{sgn}(k_a) = \operatorname{sgn}(k_b)$. By exploiting this property, the asymptotical analysis about $d_1 = d_2 = 0$ shows that in such a case $\operatorname{arctanh}(d_3/r)$ must be replaced by $\operatorname{sgn}(k_\vartheta) \log |k_\vartheta|$ in outcomes (44), (51), (52) and (61).

4.3.3. Evaluation of $\log(\zeta_2 + r)$. In view of definition (39), function $\log(\zeta_2 + r)$ is not appropriately defined for $d_1 = k_\vartheta = 0$. Such a condition defines the lines of the two sides of T_j emanating from the center of the coordinate system (see Figure 5). It can be seen from Figure 6 that $\mathbf{x} \notin \partial T_j$ implies $\operatorname{sgn}(d_2)$ is constant for any d_3. By exploiting this property, the asymptotical analysis about $d_1 = k_\vartheta = 0$ shows that in such a case $\log(\zeta_2 + r)$ must be replaced by $\operatorname{sgn}(d_2) \log |d_2|$ in outcomes (44), (51), (52), and (61).

4.4. On the computational cost of analytical integrations

The interest in analytical integrations is not limited to computational efficiency; nevertheless, as they in principle provide machine-precision accuracy, 'measuring' their computational cost is a primary concern. A key point to this aim is envisaging a unit of measurement independent of the computing machine, on the implemented code, on the programming language and also on the

DOI: 10.1002/nme

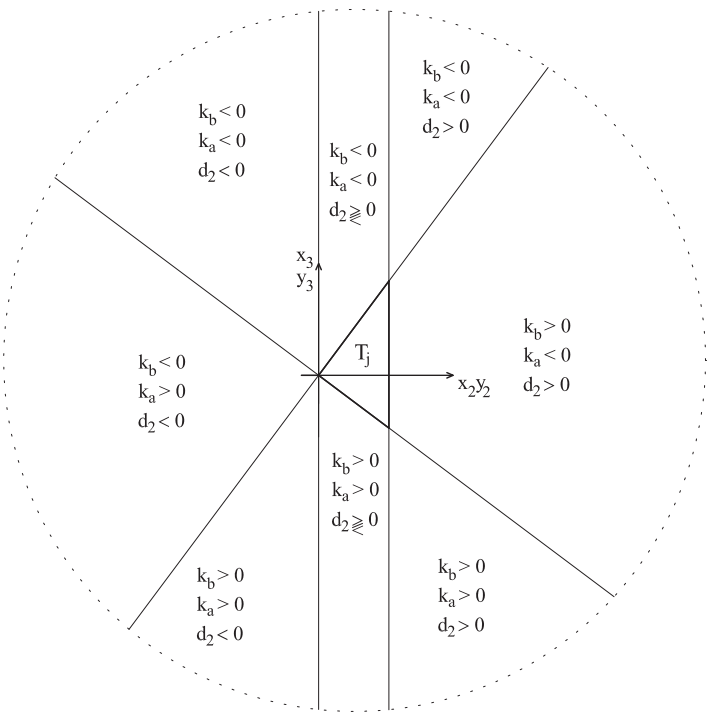

Figure 6. Different values of d_2 and k_ϑ depending on the position of point **x**.

Table II. A measure of the computational cost of the proposed analytical integrations for the Laplace equation. Indeed results for Lamé operator looks a bit better, because computational effort in (24) seems to be mainly due to scalar functions (log, arctan).

	$\mu(G_{uu})$	$\mu(G_{up})$	$\mu(G_{pu})$	$\mu(G_{pp})$
x co-planar with T_j	6	—	—	6.16
x out of plane	7.06	6.22	6.53	7.13

compiler: a very hard task to cope with. The computational cost $\mu(G_{rs})$ of analytical integrations (22) has been measured against the evaluation of kernel G_{rs}:

$$\mu(G_{rs}) = \sqrt{\frac{\mathbb{K}_{rs} \text{ elapsed time}}{G_{rs} \text{ elapsed time}}} \tag{74}$$

Such a measure does not depend on the hardware, but it does on the implementation. The results relevant to the Laplace equation are collected in Table II.

DOI: 10.1002/nme

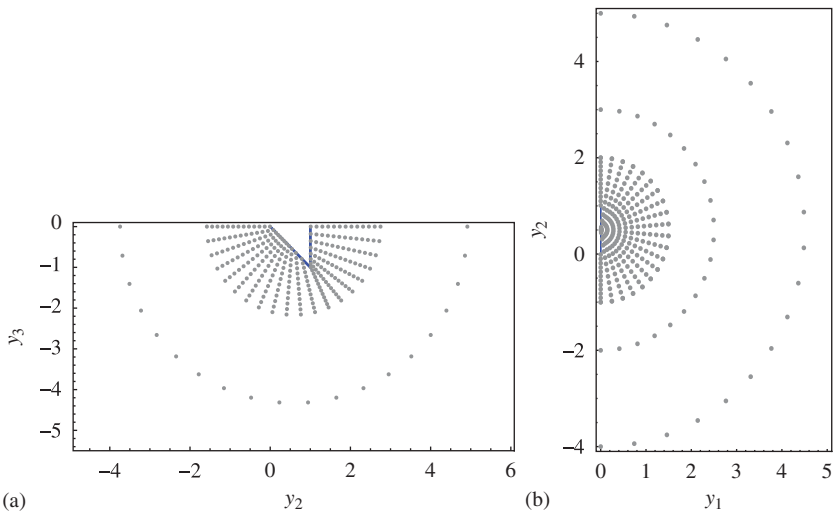

Figure 7. Set of field points **x** for the iso-Gauss points maps of Figures 8 and 9. The set for the far field is made of points that belong to semi-circumferences of radius $r=2^k r_0$, with r_0 the distance between the lower vertex and the incenter of the triangle; $k=1, 2, 3, 4$. The near field point set is fully depicted.

Measure (74) can be significantly related to the number of nodes $n_{\mathbb{Q}}(\mathbf{x})$ of a quadrature rule $\mathbb{Q}_{rs}(\mathbf{x})$ eventually used to approximate integral (22). Comparisons must be made with respect to a target accuracy

$$\left\| \frac{\mathbb{Q}_{rs}(\mathbf{x}) - \mathbb{K}_{rs}(\mathbf{x})}{\mathbb{K}_{rs}(\mathbf{x})} \right\| < \zeta$$

The higher the accuracy, the higher the $n_{\mathbb{Q}}(\mathbf{x})$, obviously. The number of nodes $n_{\text{Gauss}}(\mathbf{x})$ of a Gaussian standard quadrature rule

$$\int_0^{\overline{y}_2} \int_{a\,y_2}^{b\,y_2} g(y_2, y_3)\,\mathrm{d}y_3\,\mathrm{d}y_2 \approx \frac{\overline{y}_2{}^2}{8}(b-a) \sum_{k=1}^{n_{\text{Gauss}}} w_k(1+x_k) \sum_{i=1}^{n_{\text{Gauss}}} w_i\, g(y_2(x_k), y_3(x_i, x_k))$$

is depicted in Figures 8 and 9. They map $n_{\text{Gauss}}(\mathbf{x})$ required to reach accuracy $\zeta = 10^{-6}$ at field point **x**. The set of nodes where kernels G_{uu} and G_{pp} have been evaluated is plotted in Figure 7. The panel T_j of integral (22) is depicted as well.

In terms of efficiency, analytical integrations are comparable to a Gauss quadrature in the far field, whereas the usage of analytical formulae seems to be useful in the near-field. Additional work will take into account the several quadrature rules—some of which are extremely recent [39]—available in the literature.

4.5. Benchmarks

The following benchmarks aim at showing the capability of the analytical formulation proposed. They pertain to the 'hypersingular collocation' scheme, whose limitation and drawbacks are well known; the goal is merely to show the effectiveness of the integration strategy, not of the numerical scheme: the analysis and the implementation of the Galerkin approach is in progress and will be considered in a forthcoming publication.

DOI: 10.1002/nme

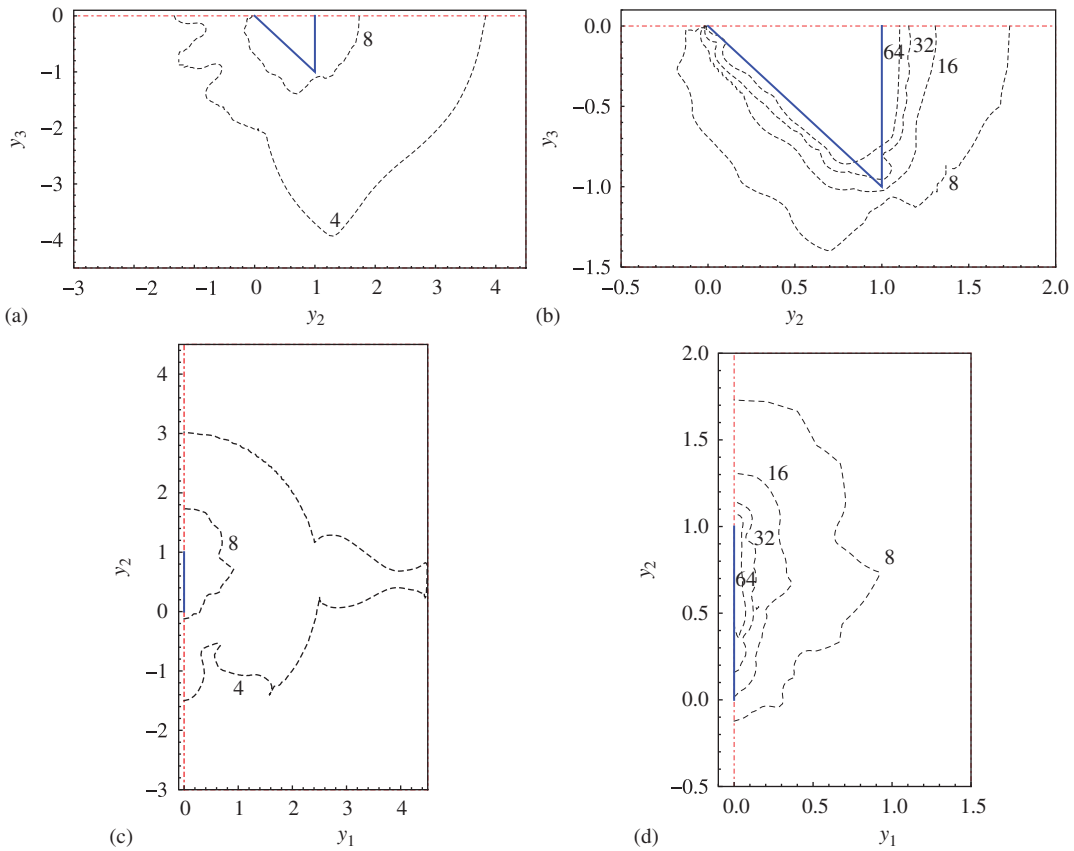

Figure 8. Number of nodes $n_{\text{Gauss}}(\mathbf{x})$ required to reach accuracy $\zeta = 10^{-6}$ for a Gauss rule for the quadrature of kernel G_{uu} for the Laplace operator. Pictures (a) and (b) refer to the plane $y_1 = 0$ and might be compared with the first row of Table II. The picture is plotted exploiting symmetry of the involved fields about axes $y_3 = 0$. Pictures (c) and (d) refer to the plane $y_3 = 0$ and might be compared with the second row of Table II. Contour line crosses the triangle in Figure (b) because of the interpolation algorithm: indeed $n_{\text{Gauss}}(\mathbf{x})$ has been evaluated onto the set of points of Figure 7.

Laplace operator on a cube: Consider the harmonic function $f(\mathbf{x}) = x_3(x_1^2 - x_2^2)$. An approximation of $f(\mathbf{x})$ is sought for on a cube of side $L = 20$ centered at the origin of the coordinate system, assuming linear shape functions for potential and fluxes. A mixed boundary value problem is set up, by constraining one quarter of a cube side. Four different meshes, recursively obtained by the Sierpinsky map on the cube sides, are described in Figure 10; as a property of the Sierpinsky map, the radius of the circumcircle, assumed as triangulation parameter, geometrically decreases with the recursion index $h = L/2^{\text{rec}}$ and the number of elements is related to h as $\text{El} = (24/L^2)h^2$.

Accuracy of the scheme is measured in several norms. Displacement and gradients have been evaluated at a set of points $P_j = \{j, 0, j\}$, $j = 1, 2, \ldots, 9$ and errors $\varepsilon_j^u = |u_h(P_j) - f(P_j)|/|f(P_j)|$

DOI: 10.1002/nme

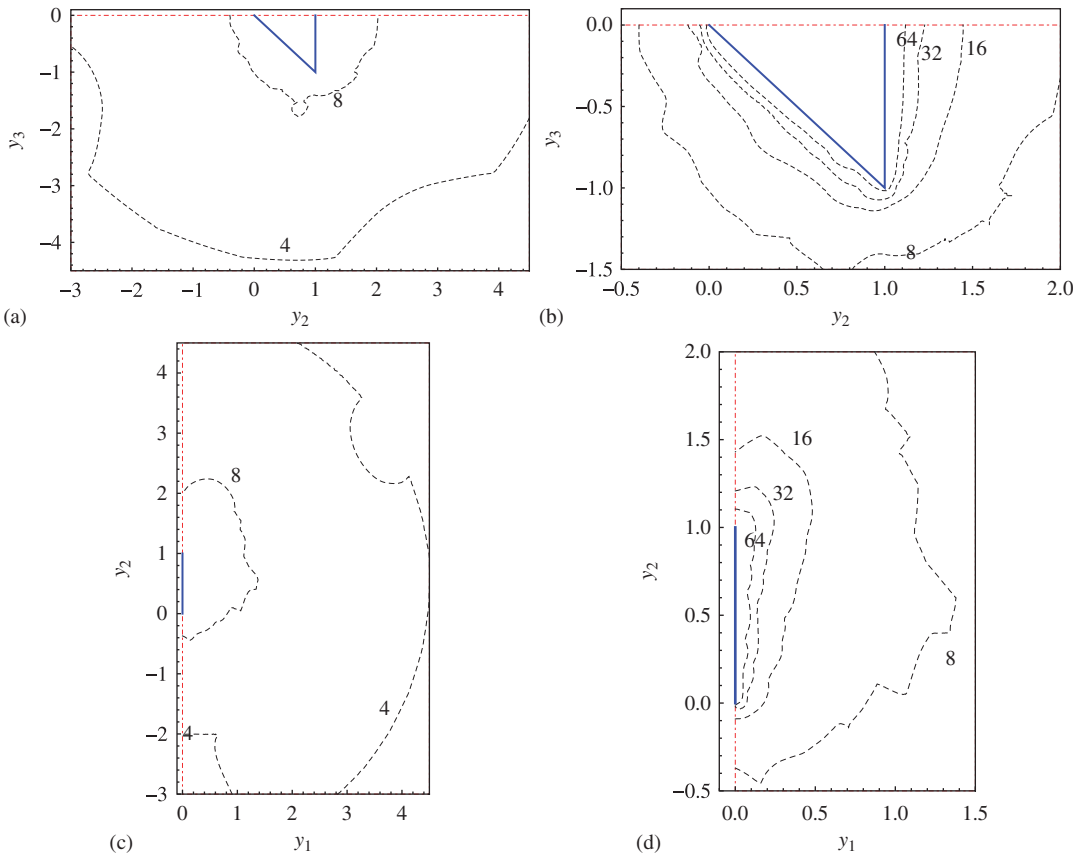

Figure 9. Number of nodes $n_{\text{Gauss}}(\mathbf{x})$ required to reach accuracy $\zeta = 10^{-6}$ for a Gauss rule for the quadrature of kernel G_{pp} for the Laplace operator. Pictures (a) and (b) refer to the plane $y_1 = 0$ and might be compared with the first row of Table II. The picture is plotted exploiting symmetry of the involved fields about axes $y_3 = 0$. Pictures (c) and (d) refer to the plane $y_3 = 0$ and might be compared with the second row of Table II.

for potential and $\varepsilon_j^p = \|p_h(P_j) - \alpha\nabla f(P_j)\| / \|\alpha\nabla f(P_j)\|$ for gradient** are plotted in Figure 11; values for $j = 1, 5, 9$ are tabulated in Tables III and IV. Convergence is envisaged, but its rate appears to be hardly measurable from ε_j^u and ε_j^p.

The relative error in L_2 norm for the Dirichlet and the Neumann data

$$\varepsilon_{L_2}^u = \frac{\|u_h(\mathbf{x}) - f(\mathbf{x})\|_{L_2(\Gamma_p)}}{\|f(\mathbf{x})\|_{L_2(\Gamma_p)}}, \quad \varepsilon_{L_2}^p = \frac{\|p_h(\mathbf{x}) - \alpha\nabla f(\mathbf{x})\cdot\mathbf{n}\|_{L_2(\Gamma_u)}}{\|\alpha\nabla f(\mathbf{x})\cdot\mathbf{n}\|_{L_2(\Gamma_u)}} \tag{75}$$

is reported in Table V together with error ε_E in bilinear form (8). Denoting with $y^{\mathsf{T}} = [f(\mathbf{x}), \alpha\nabla f(\mathbf{x})\cdot\mathbf{n}]$ the exact solution and with y_h the hypersingular collocation approximation,

**Here $\|g\| = \sqrt{g\cdot g}$ and α is the material constitutive parameter that relates fluxes to potential (e.g. conductivity for heat transfer).

DOI: 10.1002/nme

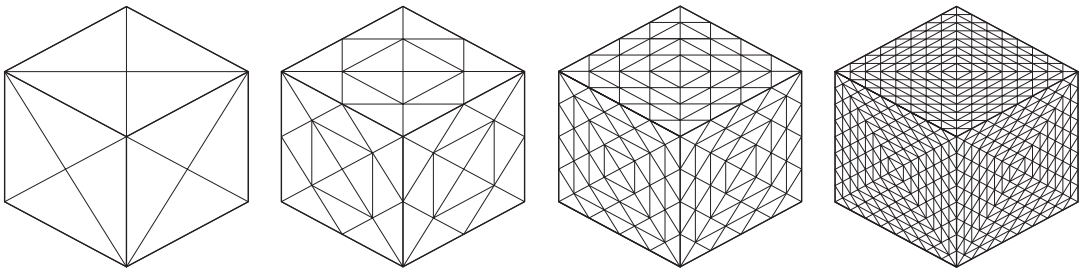

Figure 10. Four different meshes, recursively obtained with the Sierpinsky application on the cube sides. Further data are printed in Table III.

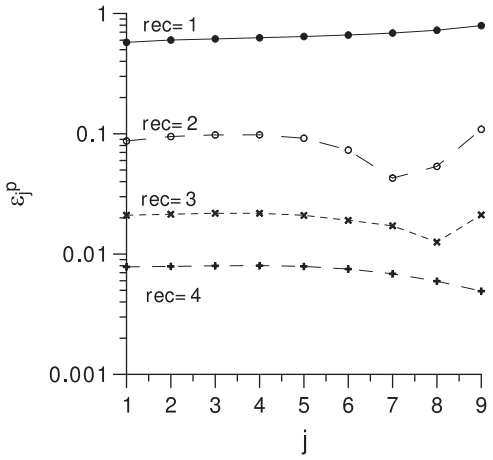

Figure 11. A wider spectra for the gradient error $\varepsilon_j^p = |p_h(P_j) - \alpha\nabla f(P_j)|/|\alpha\nabla f(P_j)|$ with respect to Table IV.

Table III. Comparison of different meshes. rec stands for the recursion index, N for the number of nodes, El for the number of elements, h for the radius of elements circumcircle, L for cube side (in the analysis taken as $L=20$), ε_j for the relative error at point P_j and CR_j is the convergence rate at point P_j.

rec	N	El	h	ε_1^u	CR_1	ε_5^u	CR_5	ε_9^u	CR_9
1	14	24	L	5.43E−1	—	6.34E−1	—	7.24E−1	—
2	50	96	$L/2$	4.69E+0	0.12	6.21E−2	10.21	2.28E−3	317.13
3	194	384	$L/4$	8.05E−1	5.82	1.59E−2	3.92	1.19E−2	0.19
4	770	1536	$L/8$	1.42E−1	5.68	9.27E−3	1.71	7.28E−3	1.63

Note that $O(\mathrm{El}) = O(h^2)$. The displacement error measured by ε_j^u is also reported.

DOI: 10.1002/nme

Table IV. The gradient error measured by ε_j^p at points P_j.

rec	N	El	h	ε_1^p	CR_1	ε_5^p	CR_5	ε_9^p	CR_9
1	14	24	L	5.75E−1	—	6.43E−1	—	7.92E−1	—
2	50	96	$L/2$	8.71E−2	6.61	9.17E−2	7.01	1.09E−1	7.27
3	194	384	$L/4$	2.10E−2	4.15	2.10E−2	4.37	2.11E−2	5.15
4	770	1536	$L/8$	7.83E−3	2.68	7.89E−3	2.66	4.92E−3	4.3

Table V. The error measured by $\varepsilon_{L_2}^u$, $\varepsilon_{L_2}^p$ and ε_E.

rec	N	El	h	$\varepsilon_{L_2}^u$	$CR_{L_2}^u$	$\varepsilon_{L_2}^p$	$CR_{L_2}^p$	ε_E	CR_E
1	14	24	L	1.00E+00	—	2.60E−01	—	1.00E+00	—
2	50	96	L/2	1.96E−01	5.10	5.40E−02	4.81	1.41E−01	7.11
3	194	384	L/4	4.60E−02	4.26	1.90E−02	2.84	3.11E−02	4.52
4	770	1536	L/8	1.40E−02	3.29	9.20E−03	2.07	1.16E−02	2.68

ε_E is defined as

$$\varepsilon_E = \frac{\mathscr{A}_{\mathscr{L}}((y-y_h),y)}{\mathscr{A}_{\mathscr{L}}(y,y)} = \frac{\int_{\Gamma_u}(p_h(\mathbf{x})-\alpha\nabla f(\mathbf{x})\cdot\mathbf{n})f(\mathbf{x})\,\mathrm{d}\Gamma+\int_{\Gamma_p}(u_h(\mathbf{x})-f(\mathbf{x}))\alpha\nabla f(\mathbf{x})\cdot\mathbf{n}\,\mathrm{d}\Gamma}{\int_{\partial\Omega} f(\mathbf{x})\alpha\nabla f(\mathbf{x})\cdot\mathbf{n}\,\mathrm{d}\Gamma} \tag{76}$$

It is worth noting that bilinear form (8) is not positive definite, but that $\mathscr{A}_{\mathscr{L}}(y,y)\geqslant 0$, what comes out also from the internal energy meaning of $\mathscr{A}_{\mathscr{L}}$ at problem solution y.

Lamé operator on an icosahedron: This benchmark is devoted to Navier's equation:

$$G\Delta\mathbf{u}(\mathbf{x})+(\lambda+G)\nabla\,\mathrm{div}\mathbf{u}(\mathbf{x})=0,\quad \mathbf{x}\in\Omega \tag{77}$$

with G and λ denoting the Lamé constants. They are taken as independent of $\mathbf{x}$, namely material is taken as homogeneous in domain Ω. The latter is assumed to be an icosahedron.

Consider displacement field

$$\mathbf{u}(\mathbf{x})=\mathbf{x} \tag{78}$$

which is a solution of (77). The stress tensor relevant to (78) reads as

$$\boldsymbol{\sigma}(\mathbf{x})=\frac{E}{1-2v}\mathbb{1} \tag{79}$$

where $\mathbb{1}$ denotes the identity matrix, E is Young's modulus and v is the Poisson coefficient. Traction vector at point $\mathbf{x}$ acting on a surface of normal $\mathbf{n}(\mathbf{x})$ is given by

$$\mathbf{p}(\mathbf{x},\mathbf{n}(\mathbf{x}))=\boldsymbol{\sigma}(\mathbf{x})\mathbf{n}(\mathbf{x})=\frac{E}{1-2v}\mathbf{n}(\mathbf{x}) \tag{80}$$

A mixed boundary value problem has been set imposing (78) as a Dirichlet boundary condition on boundary $\Gamma_u\subseteq\Gamma$ and (80) as a Neumann boundary condition on boundary $\Gamma_p\subset\Gamma$; boundary Γ is taken such that $\Gamma_u\cup\Gamma_p=\Gamma$ and $\Gamma_u\cap\Gamma_p=\emptyset$. Several combinations of Γ_u and Γ_p have been tested.

DOI: 10.1002/nme

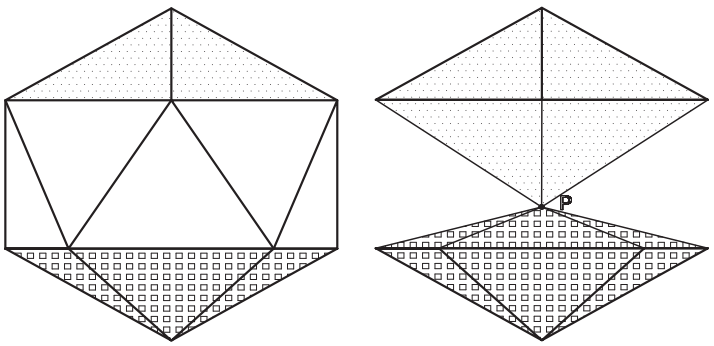

Figure 12. The domain used for the multizone linear elasticity benchmark.

It is expected that the BEM approximation by means of linear shape functions recovers the exact solution, because integrations have been analytically solved. In all simulations that have been performed, the numerical approximation showed an accuracy of at least 13 digits.

The Lamé benchmark has been made less trivial by considering different materials (see Figure 12(a)). Each material has been taken as homogeneous, with constants:

$$\nu_n = 0.1n, \quad E_n = 1 - 2\nu_n, \quad n = 1, 2, 3 \tag{81}$$

The stress tensor relevant to displacement field

$$\mathbf{u}_n(\mathbf{x}) = \mathbf{x} \tag{82}$$

amounts to the identity matrix for all $n = 1, 2, 3$. Therefore, traction vector relevant to (82) at point $\mathbf{x}$ acting on a surface of normal $\mathbf{n}(\mathbf{x})$ is given by $\mathbf{p}_n(\mathbf{x}, \mathbf{n}(\mathbf{x})) = \mathbf{n}(\mathbf{x})$ for all $n = 1, 2, 3$.

A mixed boundary value problem has been set up imposing (82) as a Dirichlet boundary condition together with $\mathbf{p}_n(\mathbf{x}, \mathbf{n}(\mathbf{x})) = \mathbf{n}(\mathbf{x})$ as a Neumann boundary condition. The multizone boundary integral problem has been formulated according to [40] and solved. Three isotropic bodies Ω_n have been rigidly connected, i.e. neither opening nor sliding has been allowed at the interfaces. Two of them are depicted in Figure 12(b), whereas the third covers the excluded volume. Several combinations of Γ_u and Γ_p have been tested.

In all simulations that have been performed, the numerical approximation of $\mathbf{u}_n(\mathbf{x}) = \mathbf{x}$ at several field points $\mathbf{x} \in \Omega_n$ showed an accuracy higher than 13 digits.

4.6. Final remarks

In the present note, analytical integrations have been performed for BIEs (4)–(5) in their discrete form; both the singular and the regular part have been considered, so that the closed form is obtained as a function of the collocation point. The proposed outcomes are exhaustive for the collocation approach as well as for the post-process reconstruction of primal and dual fields (temperature and flux, displacement and stress). It seems to be of interest for the Galerkin technique as well, because it firmly distinguishes all the terms (emphasis must be given on the the weakly singular ones) relevant to the outer integral; the approach pursued in [36] maps the road to show the mutual cancelation of the singular terms in the outer integration process. Analytical integration for static (steady-state) problems is also the main ingredient for the evaluation of closed forms of integrals

DOI: 10.1002/nme

pertaining to time-dependent problems, such as elastodynamics and acoustics, which have been recently considered [41].

The availability of the closed form for the approximated primal and dual fields entails the possibility of analytical manipulations—see e.g. [42]. Indeed, closed forms (44), (51), (52) and (61) allow the extension to 3D fracture mechanics of the important result of Gray and Paulino [43]: in a nutshell, it has been shown that—as it happens in two dimensions—the linear term of the expansion of crack opening and sliding about the crack tip vanishes. The argument of the proof is that a linear term in such an expansion induces a logarithmic singularity for stresses at the crack front that is not compatible with the asymptotical behavior of the stress field. Details will be published in a further publication.

5. CONCLUSIONS

Analytical evaluation of 'integrals' pertaining to the BEM has been provided. It is relevant to the collocation BEM technique (11) as well as to the inner integral of symmetric Galerkin BEM (12), after performing a tessellation of the boundary by means of flat triangles. Shape functions $\phi_n(\mathbf{y})$ have been taken as polynomials of arbitrary degree: this allows—in the non-unusual case of flat surfaces (see e.g. [44])—a p-refinement technique.

Integrations have been performed in a local coordinate system, which was detailed in Section 2.1. All significant instances of the position of the source point have been analyzed. In particular, when point $\mathbf{x}$ belongs to triangle T_j, the integral does not exist in a classical sense. In such cases, the continuity (with respect to the source point) between the HFP and the Lebesgue integral has been shown. To this aim, the HFP has been directly evaluated as first; further, the limit process to the boundary $\Omega \ni \mathbf{x} \to \mathbf{x} \in \Gamma$ has been performed.

The implementation requires particular care in some pathological configurations. Section 4.3 has been devoted at describing code development details. Some benchmarks have been proposed in Section 4.5, with the mere aim of verifying the capabilities of the proposed analytical integrations and their efficiency.

Broader impacts may result from the present note: on the educational side, introductory courses in the BIEs may benefit from the closed form for Equations (4)–(5), which may lighten the burden of numerical approximation of elliptic problems via BEM to inexpert auditors.

APPENDIX A: GREEN'S FUNCTIONS

The expressions of Green's functions for 3D Laplace and linear elasticity follow. Here $\mathbf{n}(\mathbf{x})$ and $\mathbf{l}(\mathbf{y})$ are the normals at the boundary at $\mathbf{x}$ and $\mathbf{y}$, respectively. Vectors $\mathbf{d}$ and $\mathbf{r}$ are defined as $\mathbf{d} = -\mathbf{r} = (\mathbf{y} - \mathbf{x})$.

A.1. Laplace equation

$$G_{uu}(\mathbf{r}) = \frac{1}{4\alpha\pi}\frac{1}{r}$$

$$G_{pu}(\mathbf{r}; \mathbf{n}(\mathbf{x})) = -\frac{1}{4\pi}\frac{\mathbf{r}\cdot\mathbf{n}}{r^3}$$

DOI: 10.1002/nme

$$G_{up}(\mathbf{d};\mathbf{l}(\mathbf{y})) = \frac{1}{4\pi}\frac{\mathbf{r}\cdot\mathbf{l}}{r^3}$$

$$G_{pp}(\mathbf{r};\mathbf{n}(\mathbf{x});\mathbf{l}(\mathbf{y})) = -\frac{\alpha}{4\pi}\frac{1}{r^3}\left(3\frac{(\mathbf{r}\cdot\mathbf{l})(\mathbf{r}\cdot\mathbf{n})}{r^2} - \mathbf{n}\cdot\mathbf{l}\right)$$

A.2. Linear elasticity

$$\mathbf{G}_{uu}(\mathbf{d}) = \frac{1}{16\pi}\frac{1}{G(1-\nu)}\frac{1}{r}\left(\frac{\mathbf{d}\otimes\mathbf{d}}{r^2} + (3-4\nu)\mathbf{I}\right)$$

$$\mathbf{G}_{pu}(\mathbf{d};\mathbf{n}(\mathbf{x})) = -\frac{1}{8\pi}\frac{1}{(1-\nu)}\frac{1}{r^3}\left[(1-2\nu)(2\mathbf{SKW}(\mathbf{d}\otimes\mathbf{n}) - (\mathbf{d}\cdot\mathbf{n})\mathbf{I}) - 3(\mathbf{d}\cdot\mathbf{n})\frac{\mathbf{d}\otimes\mathbf{d}}{r^2}\right]$$

$$\mathbf{G}_{up}(\mathbf{d};\mathbf{l}(\mathbf{y})) = -\frac{1}{8\pi}\frac{1}{(1-\nu)}\frac{1}{r^3}\left[(1-2\nu)(2\mathbf{SKW}(\mathbf{d}\otimes\mathbf{l}) + (\mathbf{d}\cdot\mathbf{l})\mathbf{I}) + 3(\mathbf{d}\cdot\mathbf{l})\frac{\mathbf{d}\otimes\mathbf{d}}{r^2}\right]$$

$$\begin{aligned}\mathbf{G}_{pp}(\mathbf{d};\mathbf{n}(\mathbf{x});\mathbf{l}(\mathbf{y})) = \frac{G\nu}{4\pi(1-\nu)}\frac{1}{r^3}\Bigg\{&2\mathbf{SYM}(\mathbf{l}\otimes\mathbf{n}) + 2\mathbf{SKW}(\mathbf{l}\otimes\mathbf{n})\frac{3\nu-1}{\nu}\\ &+3\frac{(3\nu-1)}{\nu}\left[\mathbf{SKW}(\mathbf{d}\otimes\mathbf{l})\frac{\mathbf{d}\cdot\mathbf{n}}{r^2} - \mathbf{SKW}(\mathbf{d}\otimes\mathbf{n})\frac{\mathbf{d}\cdot\mathbf{l}}{r^2}\right]\\ &+3\frac{(1-\nu)}{\nu}\left[\mathbf{SYM}(\mathbf{d}\otimes\mathbf{l})\frac{\mathbf{d}\cdot\mathbf{n}}{r^2} + \mathbf{SYM}(\mathbf{d}\otimes\mathbf{n})\frac{\mathbf{d}\cdot\mathbf{l}}{r^2}\right]\\ &+3\frac{\mathbf{d}\otimes\mathbf{d}}{r^2}\left[(\mathbf{l}\cdot\mathbf{n}) - \frac{5}{\nu}\frac{(\mathbf{d}\cdot\mathbf{n})(\mathbf{d}\cdot\mathbf{l})}{r^2}\right]\\ &+\left[3\frac{(\mathbf{d}\cdot\mathbf{n})(\mathbf{d}\cdot\mathbf{l})}{r^2} + (\mathbf{l}\cdot\mathbf{n})\frac{(1-2\nu)}{\nu}\right]\mathbf{I}\Bigg\}\end{aligned}$$

APPENDIX B: FUNDAMENTAL LEBESGUE INTEGRALS

The following identities, which can be proved by induction when $d_1 \neq 0$, are the keynote of the inner integration. Here, the following notation will be considered:

$\widehat{k} = k \div 2$ integer division $k \div 2$.
$k_{[2]} = k - 2\widehat{k}$ remainder of the (integer) division $k \div 2$.
$I_{\triangle}^{r^{-3}}(\mathbf{x}, d_2, d_3)$ has been defined in Section 4.2.

DOI: 10.1002/nme

Proposition
By defining with

$$\lambda(\vartheta)=\frac{1}{\vartheta^2 d_1^2+k_\vartheta^2},\qquad d_3=\vartheta d_2+k_\vartheta \tag{A1}$$

it holds

$$\int_{-x_2}^{\bar{y}_2-x_2}\frac{d_2^{n_{[2]}}}{d_1^2+d_2^2}\frac{1}{r}\bigg|_{\vartheta=a}^{\vartheta=b}\mathrm{d}d_2=\lambda(\vartheta)\left[\alpha\,\mathrm{arctanh}\frac{d_3}{r}+\beta I_{\triangle}^{r^{-3}}(\mathbf{x},d_2,d_3)\bigg|_{\vartheta=a}^{\vartheta=b}\right]_{d_2=-x_2}^{d_2=\bar{y}_2-x_2} \tag{A2}$$

$$\int_{-x_2}^{\bar{y}_2-x_2}\frac{d_2^{n_{[2]}}}{(d_1^2+d_2^2))^2}\frac{1}{r}\bigg|_{\vartheta=a}^{\vartheta=b}\mathrm{d}d_2=\lambda^3(\vartheta)\left[\gamma\,\mathrm{arctanh}\frac{d_3}{r}+\delta I_{\triangle}^{r^{-3}}(\mathbf{x},d_2,d_3)+\zeta r\bigg|_{\vartheta=a}^{\vartheta=b}\right]_{d_2=-x_2}^{d_2=\bar{y}_2-x_2} \tag{A3}$$

$$\int_{-x_2}^{\bar{y}_2-x_2}\frac{d_2^{n_{[2]}}}{(d_1^2+d_2^2))^3}\frac{1}{r}\bigg|_{\vartheta=a}^{\vartheta=b}\mathrm{d}d_2=\lambda^5(\vartheta)\left[\eta\,\mathrm{arctanh}\frac{d_3}{r}+\theta I_{\triangle}^{r^{-3}}(\mathbf{x},d_2,d_3)+\imath r\bigg|_{\vartheta=a}^{\vartheta=b}\right]_{d_2=-x_2}^{d_2=\bar{y}_2-x_2} \tag{A4}$$

where

$$\alpha=-k_\vartheta n_{[2]}+\vartheta(1-n_{[2]})$$

$$\beta=\vartheta d_1^2 n_{[2]}+k_\vartheta(1-n_{[2]})$$

$$\gamma=\frac{k_\vartheta}{2}(4k_\vartheta^2-\frac{3+2\vartheta^2}{\lambda(\vartheta)})n_{[2]}+\frac{\vartheta}{2}\left(\frac{1+2\vartheta^2}{\lambda(\vartheta)}-4k_\vartheta^2\right)(1-n_{[2]})$$

$$\delta=\vartheta\frac{d_1^2\left[d_1^2\vartheta^2(1+\vartheta^2)-3k_\vartheta^2\right]-k_\vartheta^4}{2}n_{[2]}+k_\vartheta\frac{d_1^2(3\vartheta^2 d_1^2(1+\vartheta^2)-k_\vartheta^2(1-4\vartheta^2))+k_\vartheta^4}{2d_1^2}(1-n_{[2]})$$

$$\zeta=\frac{\vartheta^2 d_1^2+2\vartheta d_2 k_\vartheta-k_\vartheta^2}{2(d_1^2+{d_2}^2)\lambda(\vartheta)}n_{[2]}-\frac{\vartheta d_1^2(\vartheta d_2-2k_\vartheta)-d_2k_\vartheta^2}{2d_1^2(d_1^2+d_2^2)\lambda(\vartheta)}(1-n_{[2]})$$

$$\eta=\frac{k_\vartheta}{8}\left(\frac{-8d_1^2\vartheta^6-8(3d_1^2+k_\vartheta^2)\vartheta^4-3(5d_1^2-8k_\vartheta^2)\vartheta^2+45k_\vartheta^2}{\lambda(\vartheta)}-48k_\vartheta^4\right)n_{[2]}$$
$$+\frac{\vartheta}{8}\left(\frac{8d_1^2\vartheta^6+8(d_1^2+k_\vartheta^2)\vartheta^4+(3d_1^2-40k_\vartheta^2)\vartheta^2-33k_\vartheta^2}{\lambda(\vartheta)}+48k_\vartheta^4\right)(1-n_{[2]})$$

$$\theta=\frac{\vartheta d_1}{8}(3\vartheta^8\,\mathrm{d}_1^5+6,\vartheta^6 d_1^5+\vartheta^4 d_1(3d_1^4-30d_1^2k_\vartheta^2-10k_\vartheta^4)$$
$$+\frac{-2\vartheta^2d_1^2(15d_1^4k_\vartheta^2+15d_1^2k_\vartheta^4+4k_\vartheta^6)+k_\vartheta^4(15d_1^4+6d_1^2k_\vartheta^2-k_\vartheta^4)}{d_1^3}\Bigg)n_{[2]}$$

DOI: 10.1002/nme

$$+\frac{k_\vartheta d_1}{8}(15\vartheta^8 d_1^5+10\vartheta^6 d_1^3(3d_1^2+4k_\vartheta^2)+\vartheta^4 d_1(15d_1^4+10d_1^2k_\vartheta^2+38k_\vartheta^4)$$

$$+\frac{\vartheta^2 d_1^2(-30d_1^4k_\vartheta^2-22d_1^2k_\vartheta^4+16k_\vartheta^6)+k_\vartheta^4(3d_1^4-2d_1^2k_\vartheta^2+3k_\vartheta^4)}{\mathrm{d}_1^5}\Bigg)(1-n_{[2]})$$

$$\iota=\frac{\vartheta^2 d_1^2+2\vartheta d_2k_\vartheta-k_\vartheta^2}{4(d_1^2+d_2^2)^2\lambda^3(\vartheta)}n_{[2]}+\frac{-\vartheta^2 d_1^2d_2+2\vartheta d_1^2k_\vartheta+d_2k_\vartheta^2}{4d_1^2(d_1^2+d_2^2)^2\lambda^3(\vartheta)}(1-n_{[2]})$$

$$+\{3\vartheta^6d_1^6+11\vartheta^5d_1^4d_2k_\vartheta+\vartheta^4(3d_1^6-6d_1^4k_\vartheta^2)+\vartheta^3(12d_1^4d_2k_\vartheta+10d_1^2d_2k_\vartheta^3)$$

$$+\vartheta^2(-18d_1^4k_\vartheta^2-9d_1^2k_\vartheta^4)+\vartheta(-12d_1^2d_2k_\vartheta^3-d_2k_\vartheta^5)+3d_1^2k_\vartheta^4\}\frac{1}{8d_1^2(d_1^2+d_2^2)\lambda(\vartheta)}n_{[2]}$$

$$+\{-6\vartheta^6d_1^6d_2+13\vartheta^5d_1^6k_\vartheta+\vartheta^4(-3d_1^6d_2+3d_1^4d_2k_\vartheta^2)+\vartheta^3(12d_1^6k_\vartheta+14d_1^4k_\vartheta^3)$$

$$+\vartheta^2(18d_1^4d_2k_\vartheta^2+12d_1^2d_2k_\vartheta^4)+\vartheta(-12d_1^4k_\vartheta^3+d_1^2k_\vartheta^5)-3d_1^2d_2k_\vartheta^4+3d_2k_\vartheta^6\}\frac{1-n_{[2]}}{8d_1^4(d_1^2+d_2^2)\lambda(\vartheta)} \quad \text{(A5)}$$

Proposition
By defining with $d_3=\vartheta d_2+k_\vartheta$ it holds

$$\int_{-x_2}^{\bar{y}_2-x_2} d_2^k\log(d_3+r)|_{\vartheta=a}^{\vartheta=b}\mathrm{d}d_2-\sum_{n=0}^{k}\varpi(n)\int_{-x_2}^{\bar{y}_2-x_2}\frac{d_2^{k-n}}{r})\Bigg|_{\vartheta=a}^{\vartheta=b}\mathrm{d}d_2$$

$$=\left[\mu\,\mathrm{arctanh}\frac{d_3}{r}+\nu I_\triangle^{r^{-3}}(\mathbf{x},d_2,d_3)+\xi\log(d_3+r)|_{\vartheta=a}^{\vartheta=b}\right]_{d_2=-x_2}^{d_2=\bar{y}_2-x_2} \quad \text{(A6)}$$

where

$$\varpi(n)=(-1)^{\widehat{n}}\frac{d_1^n}{k+1}(k_b-(k_b+bd_1)n_{[2]})$$

$$\xi=\frac{d_2^{k+1}}{k+1}$$

$$\nu=(-1)^{\widehat{k}}\frac{d_1^{k+2}}{k+1}(k_{[2]}-1)$$

$$\mu=(-1)^{\widehat{k}}\frac{d_1^{k+1}}{(k+1)}k_{[2]}$$

Proposition
With assumptions (A1) and

$$\Lambda(\vartheta)=\frac{1}{d_1^2(1+\vartheta^2)+k_\vartheta^2} \quad \text{(A7)}$$

DOI: 10.1002/nme

it holds

$$\int_{-x_2}^{\bar{y}_2-x_2} \frac{d_2^{n_{[2]}}}{d_1^2+d_2^2}\frac{1}{r^3}\bigg|_{\vartheta=a}^{\vartheta=b} \mathrm{d}d_2 = \lambda(\vartheta)\left[\rho\,\mathrm{arctanh}\frac{d_3}{r}+\varrho I_{\triangle}^{r^{-3}}(\mathbf{x},d_2,d_3)+\sigma\frac{1}{r}\bigg|_{\vartheta=a}^{\vartheta=b}\right]_{d_2=-x_2}^{d_2=\bar{y}_2-x_2} \tag{A8}$$

$$\int_{-x_2}^{\bar{y}_2-x_2} \frac{d_2^{n_{[2]}}}{(d_1^2+d_2^2)^2}\frac{1}{r^3}\bigg|_{\vartheta=a}^{\vartheta=b} \mathrm{d}d_2 = \lambda^2(\vartheta)\left[\varsigma\,\mathrm{arctanh}\frac{d_3}{r}+\tau I_{\triangle}^{r^{-3}}(\mathbf{x},d_2,d_3)+\upsilon r+\phi\frac{1}{r}\bigg|_{\vartheta=a}^{\vartheta=b}\right]_{d_2=-x_2}^{d_2=\bar{y}_2-x_2} \tag{A9}$$

where

$$\rho = \lambda^2(\vartheta)k_\vartheta(3\vartheta^2d_1^2-k_\vartheta^2)n_{[2]}+\lambda^2(\vartheta)\vartheta(-\vartheta^2d_1^2+3k_\vartheta^2)(1-n_{[2]})$$

$$\varrho = -\lambda^2(\vartheta)\vartheta d_1^2(\vartheta^2d_1^2-3k_\vartheta^2)n_{[2]}+\lambda^2(\vartheta)k_\vartheta(-3\vartheta^2d_1^2+k_\vartheta^2)(1-n_{[2]})$$

$$\sigma = \{\lambda(\vartheta)[2\vartheta^2(\vartheta^2-1)d_1^2-2\vartheta(1+\vartheta^2)d_2k_\vartheta]-\Lambda(\vartheta)[\vartheta(1+\vartheta^2)(\vartheta d_1^2-d_2k_\vartheta)]+(1-\vartheta^2)\}n_{[2]}$$
$$+\{\lambda(\vartheta)[2\vartheta((1+\vartheta^2)\vartheta d_2+(\vartheta^2-1)k_\vartheta)]-\Lambda(\vartheta)[(1+\vartheta^2)(d_2(1+\vartheta^2)+\vartheta k_\vartheta)]\}(1-n_{[2]})$$

$$\varsigma = \lambda^3(\vartheta)3k_\vartheta\frac{5\vartheta^4d_1^4+4\vartheta^6d_1^4+k_\vartheta^4-2\vartheta^2k_\vartheta^2(5d_1^2+2k_\vartheta^2)}{2}n_{[2]}$$
$$+\lambda^3(\vartheta)\vartheta\frac{-\vartheta^4(3+4\vartheta^2)d_1^4+2\vartheta^2(15+8\vartheta^2)d_1^2k_\vartheta^2+5(-3+4\vartheta^2)k_\vartheta^4}{2}(1-n_{[2]})$$

$$\tau = \lambda^3(\vartheta)3\vartheta\frac{\vartheta^4(1+\vartheta^2)d_1^6-5\vartheta^2(2+\vartheta^2)d_1^4k_\vartheta^2-5(-1+\vartheta^2)d_1^2k_\vartheta^4+k_\vartheta^6}{2}n_{[2]}$$
$$+\lambda^3(\vartheta)k_\vartheta\frac{-15\vartheta^4(1+\vartheta^2)d_1^6-5\vartheta^2(-6+\vartheta^2)d_1^4k_\vartheta^2+(-3+11\vartheta^2)d_1^2k_\vartheta^4+k_\vartheta^6}{2d_1^2}(1-n_{[2]})$$

$$\upsilon = \left\{-\lambda^2(\vartheta)4\vartheta^3d_1^2(\vartheta d_1^2+d_2k_\vartheta)+2\lambda(\vartheta)\vartheta(2\vartheta d_1^2+d_2k_\vartheta)-\frac{1}{2}\right\}\frac{n_{[2]}}{d_1^2+d_2^2}$$
$$+\left\{\lambda^2(\vartheta)4\vartheta^3d_1^2(\vartheta d_2-k_\vartheta)-2\lambda(\vartheta)\vartheta(2\vartheta d_2-k_\vartheta)+\frac{d_2}{2d_1^2}\right\}\frac{1-n_{[2]}}{d_1^2+d_2^2}$$

$$\phi = \{\lambda^2(\vartheta)8\vartheta^3d_1^2(\vartheta(-1+\vartheta^2)d_1^2-(1+\vartheta^2)d_2k_\vartheta)+\lambda(\vartheta)4\vartheta(2\vartheta(1-2\vartheta^2)d_1^2+(1+\vartheta^2)d_2k_\vartheta)$$
$$+-(1-6\vartheta^2+\vartheta^4)+\Lambda(\vartheta)\vartheta(1+\vartheta^2)^2(\vartheta d_1^2-d_2k_\vartheta)\}n_{[2]}$$
$$+\{\lambda^2(\vartheta)8\vartheta^3d_1^2(\vartheta(1+\vartheta^2)d_2+(-1+\vartheta^2)k_\vartheta)+\lambda(\vartheta)4\vartheta(k_\vartheta-\vartheta(2(1+\vartheta^2)d_2+3\vartheta k_\vartheta))$$
$$+\Lambda(\vartheta)(1+\vartheta^2)^2(d_2(1+\vartheta^2)+\vartheta k_\vartheta)\}(1-n_{[2]})$$

DOI: 10.1002/nme

Proposition
With assumptions (A1), (A7) it holds

$$\int_{-x_2}^{\bar{y}_2-x_2} \frac{d_2^{n_{[2]}}}{d_1^2+d_2^2}\frac{1}{r^5}\Bigg|_{\vartheta=a}^{\vartheta=b} \mathrm{d}d_2 = \lambda(\vartheta)\left[\varphi \operatorname{arctanh}\frac{d_3}{r}+\chi I_{\triangle}^{r^{-3}}(\mathbf{x},d_2,d_3)+\psi\frac{1}{r}+\omega\frac{1}{r^3}\Bigg|_{\vartheta=a}^{\vartheta=b}\right]_{d_2=-x_2}^{d_2=\bar{y}_2-x_2} \tag{A10}$$

where

$$\varphi=\lambda^4(\vartheta)\{-k_\vartheta(5\vartheta^4d_1^4-10\vartheta^2d_1^2k_\vartheta^2+k_\vartheta^4)n_{[2]}+\vartheta(\vartheta^4d_1^4-10\vartheta^2d_1^2k_\vartheta^2+5k_\vartheta^4)(1-n_{[2]})\}$$

$$\chi=\lambda^4(\vartheta)\{d_1^2(\vartheta^5d_1^4-10\vartheta^3d_1^2k_\vartheta^2+5\vartheta k_\vartheta^4)n_{[2]}+(5\vartheta^4d_1^4k_\vartheta-10\vartheta^2d_1^2k_\vartheta^3+k_\vartheta^5)(1-n_{[2]})\}$$

$$\begin{aligned}\psi=\lambda(\vartheta)\Bigg\{&-\lambda^2(\vartheta)8\vartheta^3d_1^2(\vartheta(-1+\vartheta^2)d_1^2-(1+\vartheta^2)d_2k_\vartheta)\\&+\lambda(\vartheta)4\vartheta(\vartheta(-2+3\vartheta^2+\vartheta^4)d_1^2-(1+\vartheta^2)^2d_2k_\vartheta)\\&-\Lambda^2(\vartheta)\frac{2\vartheta(1+\vartheta^2)^2(\vartheta d_1^2-d_2k_\vartheta)((1+2\vartheta^2)d_1^2+2k_\vartheta^2)}{3}\\&+\Lambda(\vartheta)\frac{k_\vartheta(3\vartheta(1+3\vartheta^2+2\vartheta^4)d_2+(3-5\vartheta^2-2\vartheta^4)k_\vartheta)-(-3+7\vartheta^2+18\vartheta^4+8\vartheta^6)d_1^2}{3}\Bigg\}n_{[2]}\\&+\lambda(\vartheta)\Bigg\{-\lambda^2(\vartheta)8\vartheta^3d_1^2(\vartheta(1+\vartheta^2)d_2+(-1+\vartheta^2)k_\vartheta)\\&+\lambda(\vartheta)4\vartheta(-k_\vartheta+\vartheta(2+\vartheta^2)(d_2(1+\vartheta^2)+\vartheta k_\vartheta))\\&-\Lambda^2(\vartheta)\frac{2(1+\vartheta^2)^2(d_2(1+\vartheta^2)+\vartheta k_\vartheta)((1+2\vartheta^2)d_1^2+2k_\vartheta^2)}{3}\\&-\Lambda(\vartheta)\frac{(1+7\vartheta^2+6\vartheta^4)(d_2(1+\vartheta^2)+\vartheta k_\vartheta)}{3}\Bigg\}(1-n_{[2]})\end{aligned}$$

$$\begin{aligned}\omega=\Bigg\{&\lambda(\vartheta)2\vartheta\frac{\vartheta(-1+\vartheta^2)d_1^2-(1+\vartheta^2)d_2k_\vartheta}{3}\\&+\Lambda(\vartheta)\frac{k_\vartheta(k_\vartheta+\vartheta(d_2(1+\vartheta^2)-\vartheta k_\vartheta))-(-1+\vartheta^2+2\vartheta^4)d_1^2}{3}\Bigg\}n_{[2]}\\&+\{\lambda(\vartheta)2\vartheta\frac{\vartheta(1+\vartheta^2)d_2+(-1+\vartheta^2)k_\vartheta}{3}\\&-\Lambda(\vartheta)\frac{(1+\vartheta^2)(d_2(1+\vartheta^2)+\vartheta k_\vartheta)}{3}\Bigg\}(1-n_{[2]})\end{aligned}$$

DOI: 10.1002/nme

APPENDIX C: MATRICES FOR THE POTENTIAL KERNEL

C.1. Weakly singular kernel

Making reference to the notation of formulae (43)–(44), with assumptions (A7) and $u_\vartheta = 1+\vartheta^2$, it holds

$$\mathbb{L}^{uu} = u_\vartheta^{-1/2}[\mathbb{L}^A + u_\vartheta^{-1}\mathbb{L}^C]$$

where

$$\mathbb{L}^A = \left[k_\vartheta, -\frac{\vartheta}{2}\mathrm{d}_1^2\right], \quad \mathbb{L}^C = \left[0, -\frac{\vartheta}{2}k_\vartheta^2\right]$$

and

$$\mathbb{A}^{uu} = \left[d_2, \frac{1}{2}(d_1^2+d_2^2)\right], \quad \mathbb{I}^{uu} = [-d_1^2, 0], \quad \mathbb{R}^{uu} = \left[0, \frac{k_\vartheta}{2u_\vartheta}\right];$$

C.2. Strongly singular kernels

C.2.1. Kernel G_{up}. Making reference to the notation of formulae (50)–(51) and assuming $u_\vartheta = 1+\vartheta^2$, it holds

$$\mathbb{L}^{up} = \left[0, -\frac{\vartheta d_1}{\sqrt{u_\vartheta}}\right], \quad \mathbb{A}^{up} = [0, d_1], \quad \mathbb{I}^{up} = [-d_1, 0], \quad \mathbb{R}^{up} = 0, \quad \mathbb{S}^{up} = 0$$

C.2.2. Kernel G_{pu}. Making reference to the notation of formulae (50)–(52) and assuming $u_\vartheta = 1+\vartheta^2$, it holds

$$\mathbb{L}^{pu} = u_\vartheta^{-1/2}[\mathbb{L}^A + u_\vartheta^{-1}\mathbb{L}^C]$$

where

$$\mathbb{L}^A = [\vartheta n_2 - n_3, d_1 n_1 \vartheta], \quad \mathbb{L}^C = [0, k_\vartheta(\vartheta n_3 + n_2)]$$

and

$$\mathbb{A}^{pu} = [-n_2, -d_1 n_1], \quad \mathbb{I}^{pu} = [d_1 n_1, -d_1^2 n_2], \quad \mathbb{R}^{pu} = \left[0, \frac{\vartheta n_2 - n_3}{u_\vartheta}\right], \quad \mathbb{S}^{pu} = 0$$

C.3. Hyper singular kernel

Making reference to the notation of formulae (60)–(61), with assumptions (A1), (A7) and $u_\vartheta = 1+\vartheta^2$, it holds

$$\mathbb{L}^{pp} = \left[0, \frac{n_1\vartheta}{\sqrt{u_\vartheta}}\right], \quad \mathbb{A}^{pp} = [0, -n_1], \quad \mathbb{I}^{pp} = [0, -d_1 n_2], \quad \mathbb{H}^{pp} = 0$$

$$\mathbb{S}^{pp} = \lambda(\vartheta)\Lambda(\vartheta)d_1[\mathbf{n}\cdot\boldsymbol{\alpha}, \mathbf{n}\cdot\boldsymbol{\beta}], \quad \mathbb{R}^{pp} = -\frac{\lambda(\vartheta)}{(d_1^2+d_2^2)}[\mathbf{n}\cdot\boldsymbol{\gamma}, -d_1\mathbf{n}\cdot\boldsymbol{\gamma}^\perp]$$

DOI: 10.1002/nme

where

$$\boldsymbol{\alpha} = \left[2\vartheta d_1 k_\vartheta^2 + u_\vartheta d_1(\vartheta d_1^2 + d_2 k_\vartheta),\ \vartheta u_\vartheta d_1^2 d_2 - k_\vartheta(d_1^2 + k_\vartheta^2),\ \frac{u_\vartheta d_2 + \vartheta k_\vartheta}{\lambda(\vartheta)} \right]$$

$$\boldsymbol{\beta} = \left[\vartheta u_\vartheta d_2 d_1^3 - k_\vartheta d_1 (d_1^2 + k_\vartheta^2),\ -2\vartheta^2 d_2 k_\vartheta d_1^2 - (d_1^2 + k_\vartheta^2)(\vartheta d_1^2 + d_2 k_\vartheta),\ -\frac{d_1^2 + k_\vartheta^2 + \vartheta d_2 k_\vartheta}{\lambda(\vartheta)} \right]$$

$$\boldsymbol{\gamma} = \left[\vartheta d_1^2 + d_2 k_\vartheta,\ d_1(\vartheta d_2 - k_\vartheta),\ 0 \right]$$

$$\boldsymbol{\gamma}^\perp = [-\gamma_2, \gamma_1, 0]$$

$$\mathbf{n} = [n_1, n_2, n_3]$$

ACKNOWLEDGEMENTS

Part of the present work was performed at the Oak Ridge National Laboratory, Tennessee, U.S.A.; I am grateful to Professor L. J. Gray for the opportunity of visiting and working with him. I am indebted with my students A. Temponi and F. Ferrari for their great help. I am also grate to Dr S. Fata for fruitful discussions and to Professor S. Mukherjee for his encouragement in pursuing and publishing the present note. The support of the Italian Ministry of University and Research (MIUR) under grant ex 60% − 2007: 'Analisi non lineari nella meccanica dei continui e della frattura mediante il metodo degli elementi al contorno' is gratefully acknowledged.

REFERENCES

1. Partridge PW, Wrobel LC. An inverse geometry problem for the localisation of skin tumors by thermal analysis. *Engineering Analysis with Boundary Elements* 2007; **31**:803–811.
2. Chandra A, Mukherjee S. *Boundary Element Methods in Manufacturing*. Oxford Engineering Science Series. Oxford University Press: Oxford, 1997.
3. Benallal A, Fudoli CA, Venturini WS. An implicit BEM formulation for gradient plasticity and localization phenomena. *International Journal for Numerical Methods in Engineering* 2001; **53**(8):1853–1869.
4. Liu YJ, Chen XL. Continuum models of carbon nanotube-based composites using the BEM. *Electronic Journal of Boundary Elements* 2003; **1**(2):316–335.
5. El-Awady JA, Bulent Biner S, Ghoniem NM. A self-consistent boundary element, parametric dislocation dynamics formulation of plastic flow in finite volumes. *Journal of the Mechanics and Physics of Solids* 2008; **56**:2019–2035.
6. Linkov AM, Mogilevskaya SG. Finite-part integrals in problems of three-dimensional cracks. *Notes Academy of Science USSR* 1986; **50**:841–850. In Russian; translated into English in *Applied Mathematics and Mechanics*.
7. Sirtori S, Maier G, Novati G, Miccoli S. A Galerkin symmetric boundary-element method in elasticity: formulation and implementation. *International Journal for Numerical Methods in Engineering* 1992; **35**:255–282.
8. Hong KH, Chen JT. Derivations of integral equations of elasticity. *Journal of Engineering Mechanics* (ASCE) 1988; **114**:1028–10446.
9. Bonnet M, Maier G, Polizzotto C. Symmetric Galerkin boundary element method. *Applied Mechanical Review* 1998; **51**:669–704.
10. Rjasanow S, Steinbach O. *The Fast Solution of Boundary Integral Equations*. Springer: Berlin, 2007.
11. Aliabadi MH. *The Boundary Element Method*, *Volume 2—Application to Solids and Structures*. Wiley: New York, 2002.
12. Maier G, Miccoli S, Novati G, Perego U. Symmetric boundary element method in plasticity and gradient plasticity. *Computational Mechanics* 1995; **17**:115–129.

DOI: 10.1002/nme

13. Salvadori A. Hypersingular boundary integral equations and the approximation of the stress tensor. *International Journal for Numerical Methods in Engineering* 2007; **72**:722–743.
14. Young A. A single domain BEM for 3d elastostatic crack analysis using continuous elements. *International Journal for Numerical Methods in Engineering* 1996; **39**:1265–1293.
15. Mantič V. On computing boundary limiting values of boundary integrals with strongly singular and hypersingular kernels in 3d bem for elastostatics. *Engineering Analysis with Boundary Elements* 1994; **13**:115–134.
16. Mantič V. A new formula for the c-matrix in the Somigliana identity. *Journal of Elasticity* 1993; **33**:191–201.
17. Hartmann F. The somigliana identity on a piecewise smooth surface. *Journal of Elasticity* 1981; **11**:403–423.
18. Guiggiani M. Hypersingular boundary integral equations have an additional free term. *Computational Mechanics* 1995; **16**:245–248.
19. Mantič V, Paris F. Existence evaluation of the two free terms in the hypersingular boundary integral equation of potential theory. *Engineering Analysis with Boundary Elements* 1995; **16**:253–260.
20. Vodička R, Mantič V, Paris F. On the removal of the non-uniqueness in the solution of elastostatic problems by symmetric Galerkin BEM. *International Journal for Numerical Methods in Engineering* 2006; **66**:1884–1912.
21. Cruse TA. *Boundary Element Analysis in Computational Fracture Mechanics*. Kluwer: Dordrecht, The Netherlands, 1988.
22. Aliabadi MH, Rooke DP. *Numerical Fracture Mechanics*. Kluwer: Dordrecht, 1991.
23. Cruse TA, Rizzo FJ (eds). *Computational Applications in Applied Mechanics*. ASME: New York, 1975.
24. Ligget JA, Liu PLF. *The Boundary Integral Equation Method for Porous Media Flow*. Allen and Unwin: London, 1983.
25. Portela A, Aliabadi MH, Rooke DP. The dual boundary element method: effective implementations for crack problems. *International Journal for Numerical Methods in Engineering* 1992; **33**:1269–1287.
26. Carini A, Salvadori A. Analytical integrations in 3D BEM: preliminaries. *Computational Mechanics* 2002; **28**(3–4):177–185.
27. Hadamard J. *Lectures on Cauchy's Problem in Linear Partial Differential Equations*. Yale University Press: New Haven, CT, U.S.A., 1923.
28. Schwab C, Wendland WL. Kernel properties and representations of boundary integral operators. *Mathematische Nachrichten* 1992; **156**:187–218.
29. Martin P, Rizzo F. Hypersingular integrals: how smooth must the density be? *International Journal for Numerical Methods in Engineering* 1996; **39**:687–704.
30. Zemanian AH. *Distribution Theory and Transform Analysis*. Dover: New York, 1987.
31. Guiggiani M. Formulation and numerical treatment of boundary integral equations with hypersingular kernels. In *Singular Integrals in Boundary Element Methods*, Sladek V, Sladek J (eds). Advances in Boundary Elements Series. Computational Mechanics Publications: Southampton, Boston, 1998; 85–124.
32. Gray LJ. Evaluation of singular and hypersingular Galerkin boundary integrals: direct limits and symbolic computation. In *Advances in Boundary Elements*, Sladek V, Sladek J (eds). Computational Mechanics Publisher: Southampton, Boston, 1998.
33. Gray LJ, Glaeser J, Kaplan T. Direct evaluation of hypersingular Galerkin surface integrals. *SIAM Journal on Scientific Computing* 2004; **25**:1534–1556.
34. Gray LJ, Salvadori A, Phan AV, Mantič V. Direct evaluation of hypersingular Galerkin surface integrals. ii. *Electronic Journal of Boundary Elements* 2006; **4**(3):105–130.
35. Salvadori A. Analytical integrations in 2D BEM elasticity. *International Journal for Numerical Methods in Engineering* 2002; **53**(7):1695–1719.
36. Salvadori A. Analytical integrations of hypersingular kernel in 3D BEM problems. *Computer Methods in Applied Mechanics and Engineering* 2001; **190**:3957–3975.
37. Nintcheu Fata S. Explicit expressions for 3d boundary integrals in potential theory. *International Journal for Numerical Methods in Engineering* 2009; **78**(1):32–47.
38. Carini A, Diligenti M, Salvadori A. Implementation of a symmetric boundary element method in transient heat conduction with semi-analytical integrations. *International Journal for Numerical Methods in Engineering* 1999; **46**:1819–1843.
39. Chernov A. Hp quadratures for integral operators on simplices in arbitrary dimension: algorithmic aspects. *Advances in Boundary Integral Equations and Related Topics—A Conference in Honor of G.C. Hsiao's 75th Birthday*, University of Delaware Network, Delaware, U.S.A., 2009.
40. Salvadori A. A symmetric boundary integral formulation for cohesive interface problems. *Computational Mechanics* 2003; **32**(4–6):381–391.

DOI: 10.1002/nme

41. Temponi A, Salvadori A, Bosco E, Carini A, Alsalaet J. Analytical integrations in 3d BEM elastodynamics. In *Advances in Boundary Element Techniques IX*, Aliabadi MH, Abascal R (eds). EC Ltd.: U.K., 2008. ISBN: 978-0-9547783-5-4.
42. Salvadori A, Gray LJ. Analytical integrations and SIFs computation in 2D fracture mechanics. *International Journal for Numerical Methods in Engineering* 2007; **70**:445–495.
43. Gray LJ, Paulino GH. Crack tip interpolation, revisited. *SIAM Journal on Applied Mathematics* 1998; **58**:428–455.
44. Galvin P, Dominguez J. Analysis of ground motion due to moving surface loads induced by high-speed trains. *Engineering Analysis with Boundary Elements* 2007; **31**:931–941.

DOI: 10.1002/nme